AMERICAN UNIVERSITY OF BEIRUT

NEURAL NETWORK MECHANISMS UNDERLYING THE COMBINATION-SENSITIVITY PROPERTY IN THE AUDITORY CORTEX OF SONGBIRDS

by
YARA AHMAD GHAMLOUCHE

A project
submitted in partial fulfillment of the requirements
for the degree of Master of Science
to the Biomedical Engineering Program
of the Maroun Semaan Faculty of Engineering and Architecture
and the Faculty of Medicine
at the American University of Beirut

Beirut, Lebanon
April 2022

AMERICAN UNIVERSITY OF BEIRUT

NEURAL NETWORK MECHANISMS UNDERLYING THE COMBINATION-SENSITIVITY PROPERTY IN THE AUDITORY CORTEX OF SONGBIRDS

by
YARA AHMAD GHAMLOUCHE

Approved by:

Dr. Arij Daou, Assistant professor — Advisor
Biomedical engineering Program
Maroun Semaan Faculty of Engineering and Architecture

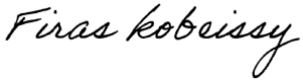

Dr. Firas Kobaissy, Associate Professor — Co-Advisor
Department of Biochemistry and Molecular Genetics
Faculty of Medicine

Jason Amatoury

Dr. Jason Amatoury, Assistant professor — Member of Committee
Biomedical engineering Program
Maroun Semaan Faculty of Engineering and Architecture

Dr. Mazen Saghir, Associate professor — Member of Committee
Department of Electrical and Computer Engineering
Maroun Semaan Faculty of Engineering and Architecture

Dr. Daniel Margoliash, Professor — Member of Committee
Department of Neuroscience
University of Chicago

Date of thesis defense: April 27, 2022

AMERICAN UNIVERSITY OF BEIRUT

THESIS RELEASE FORM

Student Name: __Ghamlouche_____Yara_____Ahmad_____
Last First Middle

I authorize the American University of Beirut, to: (a) reproduce hard or electronic copies of my thesis; (b) include such copies in the archives and digital repositories of the University; and (c) make freely available such copies to third parties for research or educational purposes:

☒ As of the date of submission

☐ One year from the date of submission of my thesis.

☐ Two years from the date of submission of my thesis.

☐ Three years from the date of submission of my thesis.

_____May 11, 2022_____

Signature Date

ACKNOWLEDGEMENTS

I would like to express my special thanks and gratitude for my advisor Dr. Arij Daou who has been guiding me every step through this thesis and at the same time, helping me grow as an academic and researcher on my own.

I would also like to thank my thesis committee members, Dr. Jason Amatoury, Dr. Firas Kobeissy and Dr. Mazen Saghir who are taking the time and effort to guide and help me make the best out of this thesis.

Lastly, I want to thank everyone who believed in me. My parents, who have supported me and stood by me through it all. And my fiancé, Hussein, who has been my main support system, encouraging me every step of the way towards achieving all my dreams since high school and till this day.

ABSTRACT
OF THE THESIS OF

Yara Ahmad Ghamlouche for Master of Science
Major: Biomedical Engineering

Title: Neural Network Mechanisms Underlying the Combination-Sensitivity Property in the Auditory Cortex of Songbirds

Temporal order of information processing in the brain is an important code in many acoustic signals including speech, music, and animal vocalizations. Despite its significance, very little is known about its underlying cellular and network mechanisms. Songbirds, among many other species are able to integrate continuous temporal information through a specialized set of neurons, known as the **combination-sensitive neurons.** These neurons respond in a facilitatory or inhibitory manner to patterns of distinct spectral elements in a signal, as long as they occur in a precise temporal order. The HVC (used as a proper name) nucleus of songbirds in particular, is the hub of many response-specific cells exhibiting the combination-sensitivity property. Although combination-sensitive neurons in the HVC are known to play a critical role in temporal auditory processing, enabling precise response selectivity to auditory signals, the underlying mechanisms of this property in the HVC are unknown. In this work, we develop conductance-based neural network models connecting the different classes of HVC neurons via different network architecture patterns with the aim of unveiling the intrinsic and synaptic mechanisms that orchestrate their combination sensitivity properties, as well as replicating their *in vivo* firing patterns observed when various auditory stimuli are presented. The model neurons in each class are designed to express pharmacologically identified ionic currents (Daou, Ross et al. 2013) and the neurons are connected via pharmacologically identified synaptic currents (Mooney and Prather 2005), rendering our network biologically plausible. We present for the first time five possible realistic scenarios in which the different types of HVC neurons can interact to produce this behavior. The result is an improved characterization of the HVC network responsible for auditory processing in the songbird system and a step forward into better understanding of temporal signal integration in the brain.

TABLE OF CONTENTS

ILLUSTRATIONS

Figure

TABLES

Table

ABBREVIATIONS

- HVC_{RA}: RA area-projecting neurons of the HVC nucleus.
- HVC_{X}: X-projecting neurons of the HVC nucleus.
- HVC_{int}: HVC interneurons.
- BOS: bird's own song
- CSN: Combination-sensitive neuron
- SMA: Supplementary motor area
- PAG: Periaqueductal gray
- DM-Ico: Dorsomedial nucleus of intercollicularis
- nRAm: Retroambigualis
- rVRG: Rostral ventral respiratory groupRA: Robust nucleus of the archistriatum
- nXIIts: Tracheosynrigeal portion of the hypoglossal nucleus
- DLM: Medial portion of the dorsolateral nucleus of the thalamus
- LMAN: Anterior neostriatum
- IPSP: Inhibitory postsynaptic potential
- dPSP: Depolarizing postsynaptic potential
- AFP: Anterior forebrain pathway
- AP: Action Potential

CHAPTER I

INTRODUCTION

Auditory perception is an intricate and organized process, being the net outcome of integration of excitatory, inhibitory, converging and diverging projections (Snyder, Gregg et al. 2012). The major function of the auditory system is to recognize sounds and create appropriate responses. Auditory research aims to achieve more detailed comprehension of the mechanisms through which we hear and identify the causes and treatments for hearing disorders. This could be achieved through attempts at understanding the intricate details of all elements of the auditory framework. A wide range of behavioral experiments in both humans (Stevens and Newman 1936, Liberman, Isenberg et al. 1981) and animals (Griffin 1958, Capranica 1965, Heiligenberg, Baker et al. 1978, Knudsen and Konishi 1979) demonstrate that a common strategy for signal identification and localization is sensitivity to two or more spectral or temporal components of a signal. This feature of the underlying neural systems is known as **combination sensitivity**. Temporal combination sensitivity is manifested in certain neurons (combination-sensitive neurons or CSNs) where action potential bursts are elicited only if the appropriate stimuli are presented in the right temporal order.

Combination sensitivity property has been extensively studied in echolocating bats (Kanwal, Matsumura et al. 1994, Nataraj and Wenstrup 2005), frogs (Fuzessery and Feng 1982, Fuzessery and Feng 1983) and songbirds (Margoliash 1983, Margoliash and Fortune 1992, Lewicki and Konishi 1995, Lewicki and Arthur 1996) among other animals. In all of these species, combination sensitivity is not restricted to a certain number of inputs nor to a fixed time interval between them (Fuzessery and Feng 1982,

Margoliash and Fortune 1992). CSNs are of different neuronal types or classes depending on the species, each having its own cellular, electrophysiological and functional properties. In songbirds, some CSNs are selective to two input syllables, others to three, and some are even selective to the presentation of all of the syllables in a song (Margoliash and Fortune 1992, Lewicki and Arthur 1996). In frogs, many auditory neurons respond only to a combination of tones either in an excitatory or inhibitory manner (Fuzessery and Feng 1983). While in bats, CSNs in the auditory cortex exhibit facilitatory responses to combinations of different frequencies in the echo and pulse, where the firing response strength depends on the interval of separation in time between the components presentation, similar to songbirds (Margoliash and Fortune 1992).

The HVC is a major cortical-like nucleus in the songbird brain that acts as a vital relay station between various nuclei and higher structures like the thalamus and auditory pathways. Neurons in the HVC are sensitive to the temporal structure of the bird's own song and are capable of integrating auditory information over several hundred milliseconds. Many of these neurons exhibit selective responses necessary for temporal integration. In HVC nucleus, forebrain projecting HVC_{RA} neurons have been shown to be nonauditory neurons (Katz and Gurney 1981, Lewicki and Arthur 1996). Basal ganglia projecting HVC_{X} neurons on the other hand, exhibit auditory selective responses that have been either excitatory or inhibitory (Lewicki and Arthur 1996). Interneurons HVC_{INT} do not exhibit auditory selectivity although they play a major role in the nucleus innervating both classes of projection neurons and orchestrating the microcircuits they are embedded in (Mooney 2000). Some neurons in the HVC are combination sensitive, where the presentation of multiple consecutive syllables in one particular order will induce a response (an excitation or an inhibition) in the combination-sensitive neuron. If one

syllable is missing or any of the consecutive syllables were presented in reversed or shuffled order, the combination sensitive neuron will not respond (Margoliash 1983, Margoliash and Fortune 1992, Lewicki and Arthur 1996).

In this work, we developed conductance-based neural network models connecting the different classes of HVC neurons with the aim to generate combination sensitivity behavior in particular HVC neurons. The neurons are modeled using pharmacologically identified ionic currents (Daou, Ross et al. 2013). Furthermore, they are connected in network architectures via previously determined synaptic currents (Mooney and Prather 2005). We developed five different fully functional networks that satisfy the appropriate conditions of combination sensitivity. We tested these models computationally and report the outcomes. For all models, we note the effect of the temperature change on the behavior of the network. Additionally, we added a delay factor to some circuit models and showed that the combination sensitivity property is maintained in the presence of consecutive stimuli that are presented with a delay of time between them, similar to what's reported experimentally (Margoliash 1983, Margoliash and Fortune 1992). We finally compare the features of all networks and discuss their biophysical accuracy. The purpose of this work is not to isolate the best network architecture that explains the combination sensitivity property but to explore different possible realistic scenarios in which the different types of HVC neurons can interact to produce this behavior.

CHAPTER II

BACKGROUND

The major function of the auditory system is to recognize sounds and create appropriate responses. Auditory research aims to achieve full comprehension of the mechanisms through which we hear and to identify the causes and treatments for hearing disorders. This could be achieved through understanding all the elements of the auditory framework. In the first relay area of the songbird brain, information carried by the cochlear nerve is delivered to numerous parallel ascending pathways that in turn project to several regions of the midbrain and brainstem and eventually converge on the HVC, creating the most notable subcortical integration center. We will start first by highlighting the similarities between songbird and mammalian species auditory systems in terms of anatomy and function, then move to focus on HVC.

A. Songbirds and Human Speech

In the study of human speech, many researchers and scholars choose to investigate the brain of songbirds because of the well-known similarities between the human's learning of speech and the bird's learning of a song. The avian song system has been the best candidate for the study of learning of speech; in both the vocal and the motor pathways (Brainard and Doupe 2002).

Unlike the majority of animals, a birdsong is not purely innate and requires learning; like the speech of human beings. While most animals are born with the ability to communicate as their species require, songbirds are taught to sing by their parents or adult figures (Doupe and Kuhl 1999).

For both birds and humans, an innate capacity as well as learning are needed in order to acquire the song or language (Konishi 1965, Marler 1970). Deaf humans and deaf birds have a lot of trouble acquiring language or song in the case of songbirds, because of the necessity of language perception and their lack of the essential experience characterized by the auditory input (Doupe 1997). Additionally, there is a critical period after birth during which learning of speech (humans) or song (songbirds) should be taking place in order to fully acquire a good and maintained communication skill for the rest of life. In fact, both species' individuals who are isolated in the critical period cannot develop good communication skills when exposed to adults later (Doupe and Kuhl 1999). Furthermore, both birdsong and speech are based on an intricate temporal and spectral structure (Theunissen and Doupe 1998). This makes the songbirds the appropriate candidates for investigating how the brain processes time-varying information. Figure 1 shows the equivalent in the human brain of the different areas of the song system.

There are other reasons beyond similarity with human speech that make the birdsong system a good system to study. Even though birdsong is a very complex behavior, the neural platform lying behind it is simple relative to the human speech system (Solis and Perkel 2005). Birdsong is a learned behavior and birds have a specialized set of interconnected nuclei that are dedicated to learning and producing of the song (Nottebohm, Stokes et al. 1976, Nottebohm, Paton et al. 1982). This and the previously stated fact that the neural substrate is relatively basic make the research on songbirds very advantageous.

Birdsong learning requires first auditory occurrences and later continuous feedback and assessment comparable with human speech (Konishi 1965, Marler 1970). There are two stages to acquiring a song. The first early stage includes the juvenile birds listening,

incorporating and memorizing the song performed by the adult. During this stage, the bird establishes a template of the song in its brain (Slater, Eales et al. 1988, Doupe 1997). The second stage includes trial and error. As it sings, the songbird sends feedback to the brain and assesses the quality of the song with respect to the template memorized. It then adjusts it accordingly (Konishi 1965). This verifies that neural auditory mechanisms exist in the brain of the songbird and that they are necessary for the learning and crystallization of the song.

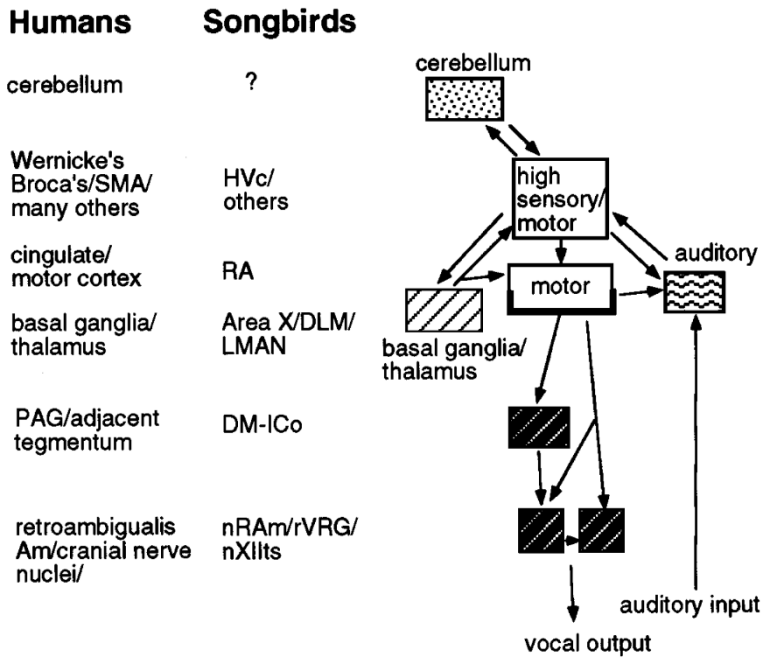

Figure 1: Schematic showing the similar hierarchy for learned vocal control is seen in both species. *Left*, different areas in the human brain and their corresponding equivalents in the songbird brain. *Right*, schematic of vocal control where the lowest areas -brainstem and midbrain controllers and integrators- (black boxes), and the motor cortex (underlined by thick black line) are shared with all non-learners. Cortex and neocortical areas (white boxes) have roles in human vocalizations; similar forebrain areas in songbirds (HVC/RA) control lower motor vocal areas in birds. Both circuits have a forebrain/basal ganglia/thalamus loop (X/DLM/LMAN in songbirds) and both circuits have auditory inputs overlapping auditory/motor centers (adopted from (Doupe and Kuhl 1999)).

B. Nucleus HVC of Songbirds

Songbirds have a special set of nuclei dedicated to the learning and to the producing of the song (Brenowitz, Margoliash et al. 1997). This set is a discrete and well-distinguished neural circuit. The system is made of two main pathways that are interconnected with well delineated and identified brain regions (Fig. 2): the descending motor pathway necessary for the motor production of a song in birds at any age (Nottebohm, Stokes et al. 1976) and the anterior forebrain pathway AFP necessary for the development and learning of the song in juvenile birds (Bottjer, Halsema et al. 1989, Luo and Perkel 1999). The descending motor pathway (Fig. 2) is composed of the nuclei including HVC area (used as a proper name), the robust nucleus of the arcopallium RA and the tracheosyringeal portion of the hypoglossal nucleus nXIIts which contains the motor neurons connected to the muscles of the avian vocal organ; the syrinx (Nottebohm, Stokes et al. 1976, Vicario and Nottebohm 1988, Vicario 1991). The second pathway is the anterior forebrain pathway (AFP, Fig. 2) and is important for processing auditory input during song modification and learning (Solis and Doupe 1997). It consists of Area X (basal ganglia), the lateral magnocellular nucleus (LMAN) and the medial nucleus of the dorsolateral thalamus (DLM). HVC nucleus is connected to the RA area directly and indirectly through the AFP by first projecting onto LMAN neurons, which are connected to the RA. RA in its role projects to all the nuclei involved with vocal motor and respiratory control (Wild 1997).

The HVC telencephalic nucleus is a cortical-like area that is responsible for the bird's singing as well as learning of his song. The HVC is a major player in the output of the song (Nottebohm, Stokes et al. 1976). In addition to its role in song production, the HVC also contributes to the learning of the song via its connections to the AFP region

(Kozhevnikov and Fee 2007). Lesioning HVC when the bird is still a juvenile learning his song will render the bird unable to continue the learning process. During singing, HVC undergoes patterned and rhythmic premotor activity (McCasland 1987) as it is responsible for the organization of the rhythm and arrangement of the series of movements (Vu, Mazurek et al. 1994).

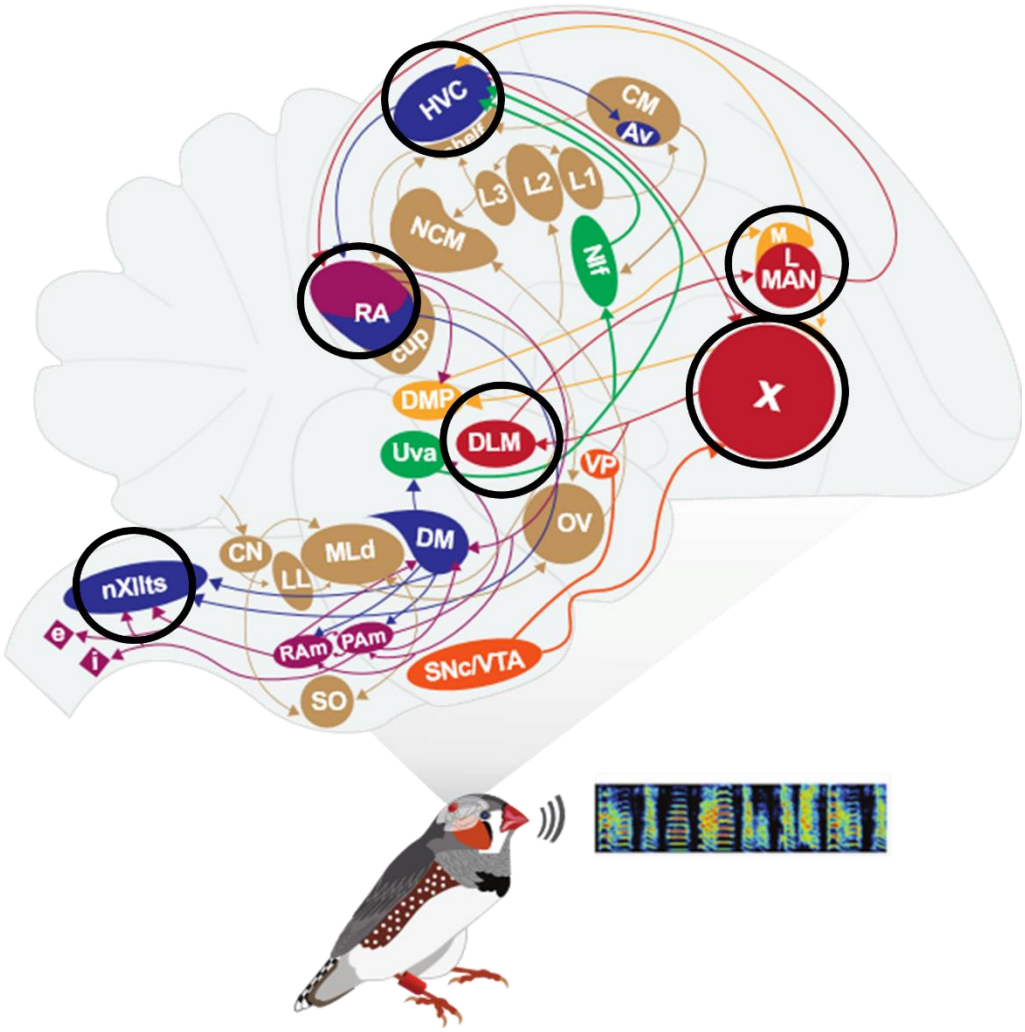

Figure 2: Schematic of the song system in songbirds. HVC (used as a proper name), RA (robust nucleus of the archistriatum) and nXIIts (the tracheosyringeal portion of the hypoglossal nucleus) are part of the descending motor pathway. The nuclei X, DLM (the medial portion of the dorsolateral nucleus of the thalamus), and LMAN (the anterior neostriatum) form a path indirectly connecting HVC to the RA (adopted from (Daou and Margoliash 2021)).

Moreover, it has been shown that *in vivo* stimulation of the HVC area causes changes in the song pattern (Vu, Mazurek et al. 1994) and that stimulation of the HVC

and RA regions can elicit vocalizations in silent birds (Vicario and Simpson 1995). Therefore, HVC is considered the hub of sensorimotor integration which relies on rhythmic neural activity (Solis and Perkel 2005). Neurons in this area are responsible for song syllables encoding (Yu and Margoliash 1996) and they are sensitive to the temporal structure of the bird's own song; capable of integrating auditory information over a period of several hundred milliseconds.

The HVC consists of three neuronal populations: basal-ganglia-projecting (HVC_X) neurons, forebrain-projecting (HVC_{RA}) neurons and interneurons (HVC_{INT}). Each type of these neurons has its own physiological and anatomical properties.

1. Auditory processing and ascending auditory pathway of songbirds:

It remains largely a mystery of how an HVC neuron perceives auditory information across multiple layers, that is, how auditory information is modulated and transformed from sound waves at the level of the ear, passing through the ascending auditory pathway, and finally to a neural code at the level of HVC where some of its neurons "understands" the signal and respond selectively to the sound wave that was played back (BOS). What is known however is that the ascending auditory pathway shares many similarities with that of mammals. Initially, air pressure signals are transduced into a neural code in the avian cochlea of the inner ear and relayed by the cochlear nuclei in the brainstem, which in their turn send their afferent axons towards the midbrain nucleus mesencephalicus lateralis pars dorsalis (MLd, homologous to the inferior colliculus). MLd sends it input to the thalamic nucleus ovoidalis (OV, homologous to the medial geniculate), which then relays its signals from the midbrain to Field L in the telencephalon (Fig.3). Field L has been divided into a number of subregions

that include: L2 which receives thalamic input and relays to L1 and L3, which in turn project to further auditory areas, including the Nidopallium caudomediale (NCM) and caudal mesopallium (CM). Although birds do not have a neocortex, it has recently been shown that the circuit organization of these telencephalic auditory areas is very similar to the layered mammalian auditory cortex (Wang, Brzozowska-Prechtl et al. 2010). Auditory processing in the inner ear and brainstem has been best described in the chicken and owl (Rubel, Smith et al. 1976, Knudsen and Konishi 1978, Carr and Konishi 1990). In songbirds, MLd, Field L, NCM, and CM are largely understudied.

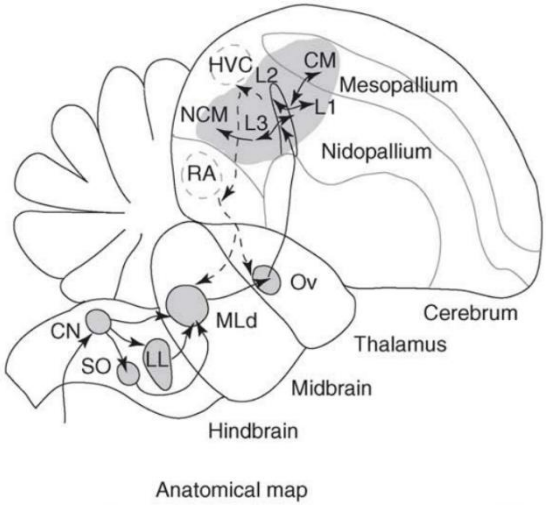

Figure 3: Schematic showing the auditory system of songbirds showing the different nuclei and NCM regions (fields L and CM) in grey in addition to other song system nuclei (CN, SO, LL, MLd and Ov) that would be found in songbirds (HVC and RA). The feed-forward pathways are shown in solid and the feedback pathway is shown with a dotted line. (adopted from (Theunissen and Shaevitz 2006))

2. Synaptic connections within HVC:

Understanding the synaptic connectivity among the three different classes is essential to dissecting the network and then building it in biologically plausible ways.

Previous studies have shown that both HVC_{RA} and HVC_X projecting neurons generate excitatory inputs to HVC_{INT} neurons that are mediated by NMDA and AMPA currents (Mooney and Prather 2005). In their turn HVC_{INT} neurons inhibit both HVC_{RA} and HVC_X via $GABA_A$ and $GABA_B$ synaptic currents (Fig. 4). Mooney and Prather (2005) found only very few monosynaptic connections between HVC_{RA} and HVC_X (Table 1), while mostly being di-synaptic inhibitory connections from HVC_{RA} neurons to HVC_X neurons via HVC_{INT} neurons. In fact, bidirectional synaptic interactions exist between these two categories of HVC neurons in a reciprocal inhibitory manner. The patterning activity in HVC is shaped by both inhibitory and excitatory synaptic inputs. The interplay between excitation and inhibition is what enables HVC_{RA}, HVC_X and HVC_{INT} neurons to generate their characteristic bursts during singing (these characteristic bursts will be highlighted in the next subsection). Most importantly, inhibitory interneurons are shown to play a major role in song production and are necessary for generating a physiological firing behavior in HVC neurons where absence of this GABA inhibition induces degradation in singing behavior (Kosche, Vallentin et al. 2015). While we know how these three classes of neurons are connected pharmacologically, how the neural network within HVC is built to generate the *in vivo* behavior that will be discussed in the very next section remains a mystery to explore.

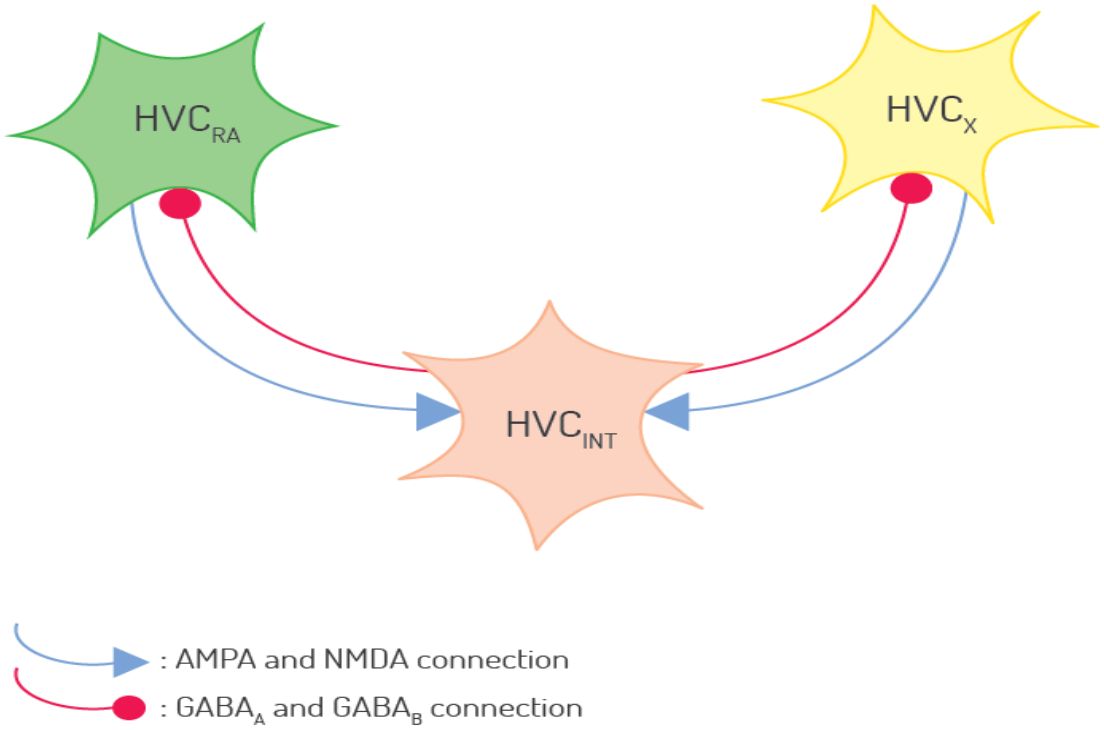

Figure 4: Cartoon diagram showing the different connectivities between the three types of HVC neurons. HVC interneurons inhibit both classes of projection neurons via GABAergic connections, which in their turn excite interneurons via AMPA and NMDA synapses.

Table 1: Frequency of cell pairs encountered in the HVC nucleus showing the different synaptic connections found between the three classes of neurons, the number of synapses found between each two and the nature of the synapse (inhibitory IPSP or excitatory dPSP) (adopted from Mooney & Prather, 2005).

Pair type	Number of pairs (percentage of total)	Number of connected pairs (percentage of pairs) [percentage total pairs]	Type of interaction (number of observations)
HVC_{RA}–HVC_{X}	46 (47.9)	6 (13) [6.25]	HVC_{RA}–HVC_{X} IPSP (4) HVC_{X}–HVC_{RA} dPSP (5) HVC_{X}–HVC_{RA} IPSP (1) Three reciprocally connected pairs
HVC_{X}–HVC_{X}	19 (19.8)	5 (26.3) [5.21]	All unidirectional IPSPs
HVC_{INT}–HVC_{X}	12 (12.5)	3 (25) [3.12]	HVC_{INT}–HVC_{X} IPSP (2) HVC_{X}–HVC_{INT} dPSP (1) One reciprocally connected pair
HVC_{RA}–HVC_{RA}	9 (9.4)	1 (11.1) [1]	Unidirectional dPSP
HVC_{RA}–HVC_{INT}	6 (6.2)	2 (33) [2]	HVC_{INT}–HVC_{RA} IPSP (1) HVC_{INT}–HVC_{RA} dPSP (1)
HVC_{INT}–HVC_{INT}	4 (4.2)	1 (25) [1]	Unidirectional IPSP
Total	96 (100%)	18 (18.7) [NA]	

3. HVC neurons activity during singing:

A groundbreaking result came from the first experiment that was able to record from HVC neurons during singing (Hahnloser, Kozhevnikov et al. 2002). In this study, they showed that HVC_{RA} neurons burst exactly once and at the same exact time during each rendition of the song (Fig. 5A). HVC_{X} neurons generate 1 to 3 bursts per song (Fujimoto, Hasegawa et al. 2011)(Fig 5B), and HVC_{INT} burst densely during singing at a very high frequency (Fig. 5A). Similar to HVC_{RA} neurons, evidence showed that HVC_{X} neurons display phase-locked patterns during singing (Fujimoto, Hasegawa et al. 2011) although they do not exhibit the same level of stereotypy as HVC_{RA} neurons. This is the most temporally precise neural sequence known in nature to date (Kozhevnikov and Fee 2007).

The extremely sparse and precise patterns of activity in HVC_{RA} and HVC_{X} neurons could suggest the entire ensemble of these two classes of projection neurons is functioning to specify the timing of syllables, notes, and even the intervening silent "gaps" between syllables. Indeed, some HVC_{RA} and HVC_{X} neurons burst during these silences, consistent with this idea (Fig. 5). If the output of the projection neurons

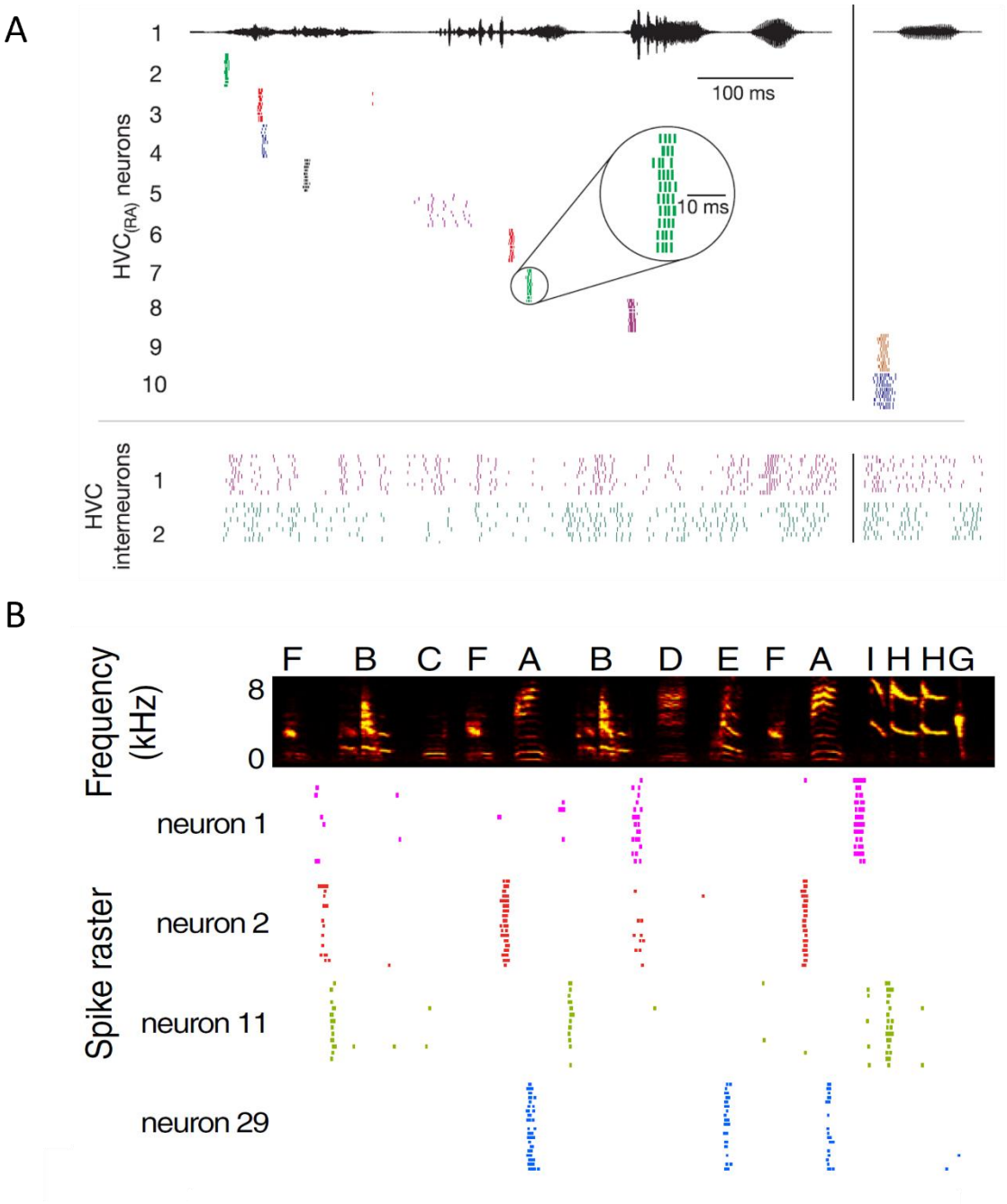

Figure 5: *A*, Song sonogram (first row) overlaid with the spike raster plot of ten different HVC_{RA} neurons and two HVC_{INT} neurons recorded in one bird during singing. Each row of ticks shows spikes generated during on rendition of the song. HVC_{RA} burst at a single precise moment in the song. HVC_{INT} burst densely throughout the song (adopted from Hahnloser et al. 2002). *B*, Spectrogram showing frequency versus time of a zebra finch song (first row). Below are the spike raster plots of 4 different HVC_X neurons recorded in one bird during singing. HVC_X neurons exhibit time-locked bursts that fire one to three times per song (adopted from Fujimoto et al. 2011).

ensemble provides a timing signal for song, what and where is the mechanism that determines and sets the song tempo and how could some of HVC neurons exhibit the sensitivity property to multiple auditory stimuli? Based on the observations that RA-projecting and X-projecting HVC neurons generate specific number of bursts during each rendition of the song motif and that different neurons appear to burst at many different times in the motif, it has been hypothesized that these neurons generate a continuous sequence of activity over time (Fee, Kozhevnikov et al. 2004, Kozhevnikov and Fee 2007). In fact, the axons of HVC_{RA} and HVC_{X} neurons extend local collaterals before exiting HVC, forming excitatory synapses with other HVC_{RA} cells, as well as interneurons and HVC_{X} cells, providing a potential substrate for a chain model (Mooney 2000, Mooney and Prather 2005, Mooney 2009, Long, Jin et al. 2010). In this case, song timing is orchestrated by the propagation of activity through the network like a chain of falling dominoes (Long, Jin et al. 2010).

4. HVC neurons in vitro activity:

Numerous *in vivo* and *in vitro* intracellular recording studies of HVC neurons have been carried out (Katz and Gurney 1981, Kubota and Saito 1991, Lewicki and Konishi 1995, Lewicki 1996, Dutar, Vu et al. 1998, Kubota and Taniguchi 1998, Schmidt and Perkel 1998, Mooney 2000, Mooney, Hoese et al. 2001, Mooney and Prather 2005, Solis and Perkel 2005, Wild, Williams et al. 2005, Long, Jin et al. 2010, Shea, Koch et al. 2010, Daou, Ross et al. 2013, Daou and Margoliash 2020). These studies shed light on several neuronal and circuit mechanisms and unveiled a variety of physiological properties within the HVC. For example, the brain slice studies demonstrated that HVC_{RA}, HVC_{X}, and HVC_{INT} neurons have distinct, categorical electrophysiological phenotypes (Dutar, Vu et

al. 1998, Kubota and Taniguchi 1998, Mooney 2000, Mooney, Hoese et al. 2001, Mooney and Prather 2005, Wild, Williams et al. 2005, Shea, Koch et al. 2010). The studies published this far have characterized HVC neurons according to their responses to depolarizing and hyperpolarizing current injections.

HVC_{RA}, HVC_X and HVC_{INT} neurons show different firing properties *in vitro*. In a nutshell, HVC_X neurons show a regular firing pattern with spike-frequency adaptation in response to depolarizing stimuli (Fig. 6A); when the neuron is depolarized with a relatively weak pulse, it starts firing at high frequency then promptly switches to a lower frequency that gradually decreases over time. This frequency adaptation had been shown pharmacologically that is due to the currents Calcium dependent K^+ current (I_{SK}) (Daou, Ross et al. 2013). In response to hyperpolarizing current pulses, HVC_X neurons show a fast and time-dependent inward rectification where a moderate sag appears in response to negative pulses (Fig. 6B). The sag is mainly due to the hyperpolarization activated inward current (I_H) while the rebound firing is mainly due to the cooperation between T-type Calcium current I_{CaT} and I_H (Daou, Ross et al. 2013). Furthermore, HVC_X neurons are silent in the absence of synaptic currents.

HVC_{RA} neurons on the other hand are known for their relative lack of excitability in response to depolarizing current pulses (Daou, Ross et al. 2013). Despite the increased magnitude of the depolarizing current pulses, the neuron usually fires one to several action potentials in response to the depolarizing pulse; this firing is usually accompanied by a long delay that's shown to be orchestrated by the A-type K+ current (I_A) (Fig. 6C, (Daou, Ross et al. 2013)). Also, HVC_{RA} generally have a much more negative hyperpolarized resting membrane potential compared to HVC_X neurons and interneurons (Fig. 6). Another key property of HVC_{RA} neurons is the absence of the sag and the

rebound firing in response to hyperpolarizing current pulses (Fig. 6D). I_A had been shown to be the main player in damping the excitability of the HVC_{RA} neuron with the cooperation of I_{SK} and I_{KNa} (Daou, Ross et al. 2013). The after-hyperpolarization current (I_{SK}) also contributes to maintaining the extremely negative resting membrane potential of these neurons. Some also suggested the presence of two physiologically distinct classes of HVC_{RA} neurons

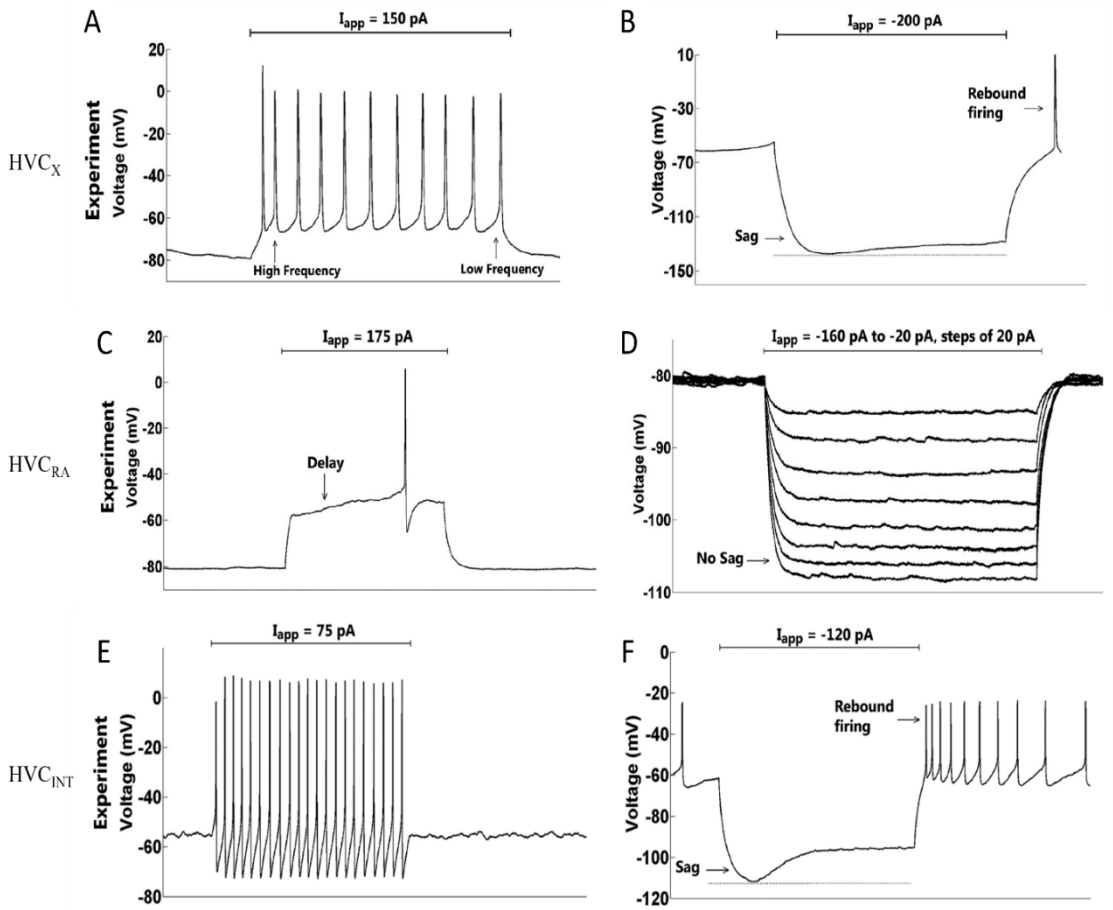

Figure 6: *In vitro* activity of HVC neurons in response to depolarizing (*Left*) and hyperpolarizing current injections (*Right*). HVC_X neuron showing exhibit spike frequency adaptation in response to positive current pulses (A) and a sag followed by a rebound burst in response to negative pulses (B). HVC_{RA} neurons exhibit a delayed and sparse firing when given a relatively large depolarizing pulse (C)and they show no sag or rebound when negative pulses are applied (D). Lastly, HVC_{INT} neurons exhibit high firing frequency in response to lower depolarizing currents with little to no adaptation (E) and they exhibit a prominent sag followed by a strong rebound burst after hyperpolarizing current pulses (F) are applied (adopted from Daou et al. 2013).

that could fire phasically or tonically in response to a depolarizing current (Shea, Koch et al. 2010).

Finally, HVC interneurons are characterized by a high firing frequency in response to depolarizing currents (Fig. 6E). Interneurons exhibit tonic firing at a high frequency with almost no spike frequency adaptation (Daou, Ross et al. 2013). Moreover they display a very prominent sag much greater than that of HVC_X neurons with a post-inhibitory rebound firing in response to hyperpolarizing current pulses (Fig. 6F). In general, HVC_{INT} neurons exhibit a resting membrane potential around -60mV while this potential falls around -72mV for HVC_X neurons and reaches its lowest value of -85mV for HVC_{RA} neurons.

Beside the classification of HVC neurons based on their ionic channels, HVC neurons have been stratified into four classes (I, IIa, IIb, III and IV) based on their different electrophysiological and morphological properties (Dutar, Vu et al. 1998, Kubota and Taniguchi 1998). Type I neurons were found to have large somata accompanied by spiny thick dendrites; most of them project to Area X. Type II neurons have been divided into two subclasses: neurons IIa have small somata and thin dendrites, while neurons IIb are characterized by their relatively large somata and thick dendrites. Type IIa neurons show similar electrical properties to HVC_{RA} neurons. Furthermore, type III neurons have beaded dendrites and exhibit tonic firing with almost no adaptation, reminiscent of HVC interneurons. Finally, type IV neurons exhibit very small somata, as well as thin, short and spiny dendrites. Some of these neurons project to RA (Kubota and Taniguchi 1998).

Various excitatory and inhibitory signals give rise to characteristic firing patterns in these neurons. Multiple lines of evidence indicates the presence of various classes of

interneurons (Wild, Williams et al. 2005) showing distinct expressions of calcium binding-proteins (parvalbumin, caldinbin, calretinin). While we know that there are multiple classes of interneurons based on the staining protocols (Wild, Williams et al. 2005), it remains an open question to know to what extent there exists in reality three different classes of HVC interneurons that exhibit different electrophysiological properties as in other rat models (Gulyás, Hájos et al. 1996, Gritti, Manns et al. 2003).

C. Combination-Sensitivity in the HVC

Selectivity is a feature of neurons observed everywhere in nature and in different species. Neuronal selectivity implies obtaining neural response only to a specific selected input. This manifests in the neuron firing one or more action potential provided the right particular stimulus. In simple terms, the right input will produce an output while any other input will have no effect.

Selectivity is observed in songbirds on many different levels. Most commonly, selectivity is evident to the bird's own song (BOS). Throughout its lifetime, each zebra finch learns and sings one specific song. This song becomes crystallized as the bird becomes an adult. Afterwards, the zebra finch will keep repeating his crystallized song forever. This song is referred to as the bird's own song (BOS). Neurons in the HVC area of the brain respond very strongly when the BOS is being played back to the bird. This response is very strong relative to any other type of auditory stimuli including pure tones and noise bursts as well as the BOS in a reverse mode - composed out of the same frequencies and features as the BOS itself - (Margoliash 1983, Lewicki and Arthur 1996, Theunissen and Doupe 1998). The fact that the reverse song does not elicit enough excitation in the neurons even though the syllables are very similar to the original ones

suggests that the neurons' response is dependent on the temporal features of the song (Doupe 1997, Solis and Doupe 1997, Theunissen and Doupe 1998). The neurons respond powerfully to the BOS by spiking to certain aspects of this song (Margoliash 1986, Volman 1996, Doupe 1997).

This selectivity is gained over time and with song learning (Volman 1996, Doupe 1997, Solis and Doupe 1997). Juvenile birds have much less selective neurons than adult birds. In fact, Solis 1997 showed that neurons had no selectivity at all for songbirds younger than 30 days old.

Auditory neurons in different areas of the songbird's brain are also selective to the BOS. Song selectivity has been observed in LMAN and X areas (Doupe and Konishi 1991, Doupe 1997) in addition to the HVC area (Margoliash 1986, Sutter and Margoliash 1994, Lewicki and Konishi 1995, Lewicki and Arthur 1996, Volman 1996, Theunissen and Doupe 1998). LMAN neurons show slightly more selectivity than X neurons. In HVC nucleus, HVC_{RA} neurons have been shown to be nonauditory neurons (Katz and Gurney 1981, Lewicki and Arthur 1996). HVC_{X} neurons on the other hand, exhibit selective responses that have been divided into depolarizing and hyperpolarizing responses (Lewicki and Arthur 1996). HVC_{INT} neurons do not exhibit song selectivity as HVCx neurons although they play a major role in the nucleus innervating both classes of projection neurons and orchestrating the microcircuits they are embedded in (Mooney 2000).

Some neurons in the HVC area are combination sensitive. This feature is a type of selectivity that is particular to more than one input. A combination sensitive neuron does not respond to one particular input alone, it responds instead to two, three or more different inputs presented in a certain temporal order. A change in the order or an absence

of one of the stimuli stops the neuron from eliciting a response. In songbirds, this is reflected by a number of syllables of the BOS. The syllables, presented in the right order only, induce an excitation or an inhibition in a combination-sensitive neuron. One missing syllable or any two syllables presented in the reversed order changes the response drastically (Margoliash 1983, Margoliash and Fortune 1992, Lewicki and Arthur 1996). This shows the temporal sensitivity and modulation of HVC neurons. Nevertheless, HVC neurons also show spectral features dependency explained by the lack of response when systematic changes are applied to the spectral features of the song (Margoliash 1983, Margoliash 1986, Mittmann and Wenstrup 1995).

Figure 7 displays the resulting number of spikes elicited by the CSN in the HVC area depending on the order and identity of the syllables being played back to the bird (Lewicki and Konishi 1995). The CSN neuron's firing rate in this example shows how it fires strongly when syllable A followed by syllable B is presented but little to no response when any of the other syllables were played back to the bird and in any other order. This begs the question of how the CSN neuron "saved" the memory of syllable A, which generally spans several hundreds of milliseconds, until syllable B is presented.

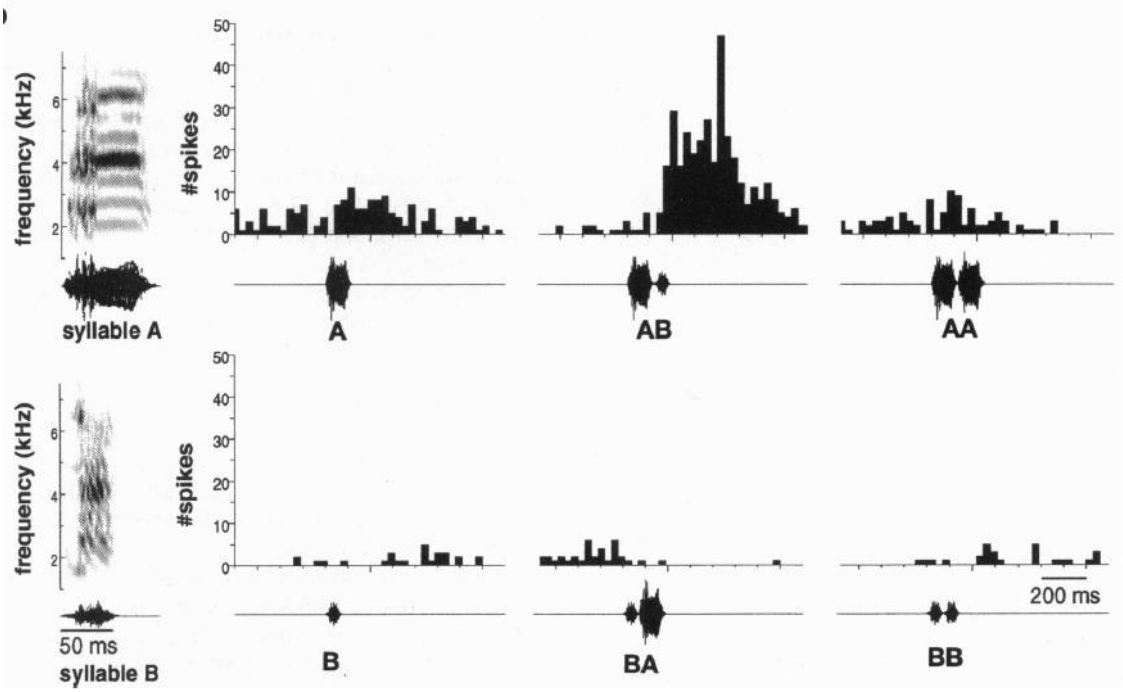

Figure 7: Temporal combination sensitivity illustrated by extracellular responses of the HVC CSN neuron. The syllables' sonograms are shown on the left. The syllables played are presented under the number of spikes in each graph. This neuron exhibits a strong response when syllable A is presented but a much stronger response when syllable A followed by syllable B is presented. It shows little to no response when B, B then A or B then B were presented (adopted from Lewicki and Konishi 1995).

Combination-sensitive neurons are not very common. They compose around 15-25% of HVC neurons (Margoliash and Fortune 1992, Lewicki and Arthur 1996). However, selective hyperpolarization responses were found to take place in almost all HVC_X neurons. Therefore, the hyperpolarization might be critical to achieve this kind of behavior (Margoliash and Fortune 1992, Lewicki and Konishi 1995, Lewicki and Arthur 1996).

It's been shown also that the latency between the onset of the last syllable of the sequence and the beginning of the response of the CSN vary dramatically, ranging from 140 to more than 340 msec (Margoliash and Fortune 1992). This latency changes depending on the environment; i.e. whether the syllables are presented solely, with other

syllables, within the song, etc. (Doupe 1997). The response also might happen at the onset, the middle or the offset of the last syllable (Margoliash and Fortune 1992). In the case of two syllables taken into consideration, if the first syllable is presented and the second syllable is delayed with an intersyllable interval – interval of time between the end of the first syllable and the presentation of the next one – of up to 325 msec in one study (Margoliash 1983) and 400 msec in another (Margoliash and Fortune 1992), the corresponding CSN neuron spikes anyway at the presentation of the second syllable. This shows that HVC neurons integrate information over many milliseconds and retain a memory of multiple stimuli to generate an auditory response.

Combination sensitive neurons exist in other species. They were discovered in the frogs' midbrain (Fuzessery and Feng 1983), in rhesus monkey (Rauschecker, Tian et al. 1995) and in the marmoset (Wang, Merzenich et al. 1995). They are also extensively studied in the inferior colliculus of echolocating bats (O'Neill and Suga 1982, Suga, O'Neill et al. 1983, Mittmann and Wenstrup 1995, Nataraj and Wenstrup 2005) in which case it was shown that inhibition plays a very crucial role in the combination sensitivity behavior (Mittmann and Wenstrup 1995, Nataraj and Wenstrup 2005) and that certain delays between frequencies - delay between first and second stimuli - produce the best responses - highest excitation level (Fuzessery and Hall 1996, Nataraj and Wenstrup 2005).

CHAPTER III

METHODOLOGY

For the purpose of understanding the mechanisms underlying the combination-sensitivity property, we divide our work to two main components. The first one being the neural circuit modeling where we sketch different wiring scenarios between the various HVC classes of neurons that would theoretically result in a combination-sensitive output from the CSN present in each network model. In the second part, we model these networks using mathematical equations that are based on Hodgkin-Huxley neuron models and on appropriate identified synaptic inhibitory and excitatory currents to report their output. These models are then tested under temperature change and different syllables durations using an additional mathematical factor that we describe in this section.

A. Neural Circuit Modeling

In order to generate biophysically realistic models, we base our work on the biological background about temporal coding and combination sensitivity known in the HVC from experimental studies, in order to build reliable, complete and functional neural circuits.

First, inhibition plays a critical role in temporal coding, and the release from inhibition plays a crucial role in rhythmogenesis in many systems in the brain. In particular, postinhibitory rebound firing is a potent signal playing the role of an indicator for the termination of a signal and the propagation of activity (Kopp-Scheinpflug, Tozer

et al. 2011, Sun, Zhang et al. 2020). This is consistent with results obtained by Mooney (2000) where it was shown that, while some neurons in the HVC respond selectively in an excitatory form to BOS, other neurons have are inhibited throughout the stimulus, eliciting firing postinhibitory bursts. This feature was utilized in most of the circuits we created, where some neurons were inhibited throughout the presentation of the first stimulus (syllable), and upon the presentation of the second stimulus, the release from inhibition generated an extra depolarizing force that caused the CNS to fire. Furthermore, in the Nataraj et al., 2005 study, the authors proved that rebound bursts after inhibition and excitation signals arriving at the same moment onto two neurons in the Inferior Colliculus of bats is essential for a CS neuron to exhibit combination sensitivity. In our models, the end of one syllable results in a rebound burst after inhibition while the presentation of the next syllable will result in an excitatory selective response in a different neuron. These two signals will therefore overlap in time and have different consequences that we explore in the subsequent models we develop.

Second, the literature shows that combination sensitivity might not be a very precise but it is a very reliable phenomenon (Margoliash and Fortune 1992, Lewicki and Arthur 1996). The researchers note that even when presenting the same syllables at the same times, the CSN will might respond at a different time. The CSN has a vast interval of time from the onset of the last syllable to its offset in which it starts firing its first action potential. Additionally, the CSN will fire even if the second syllable has been delayed by few hundreds of milliseconds from the offset of the first syllable (Margoliash 1983, Margoliash and Fortune 1992). This last feature is very important for the construction of our models, because up until we created these networks, there was no clear phenomena

or description of the underlying biophysical mechanisms that are orchestrating the temporal processing of information.

Third, auditory selective responses are mostly driven by HVC_X neurons (Margoliash 1983, Doupe and Konishi 1991). HVC_X and HVC_{RA} neurons do not form many direct monosynaptic connections between them as previously noted in the background section (Mooney and Prather 2005). Therefore, three of our models incorporate only HVC_X and HVC_{INT} neurons while in two models we include all three classes of HVC neurons. The importance and role of each of the different HVC neuronal subtypes that they play in their corresponding circuit will be further discussed in the Discussion chapter.

In few studies, general plausible ideas about the circuitry of combination sensitivity were introduced. Drew and Abbott 2002 suggested a simple version of a model circuit that relies on inhibition and excitation arriving at the same time to one neuron and cancelling out; leaving the neuron neutral in the appropriate cases. This phenomenon is called temporal summation (Drew and Abbott 2002). In their model, the CSN neuron is also selective to the 2nd syllable alone, which is contradictory to the *in vivo* behavior of the CSN. Lewicki and Konishi 1995 suggested another model based on temporal summation. Their model suggests that the 1st syllable causes an inhibition on the CSN and the 2nd syllable can stop that inhibition allowing the CSN to fire. We utilized these concepts in some of our developed models.

In this work, we consider two syllable stimuli to model the combination sensitivity property in HVC neurons, similar to what had been presented experimentally (Margoliash 1983, Margoliash 1986, Margoliash and Fortune 1992, Lewicki and Konishi 1995,

Lewicki and Arthur 1996). We call the first syllable A and the second syllable B. Our CSN is selective to the combination A-B in which A is presented first and B follows. We call the CSN neuron then an AB-selective neuron. This neuron is not selective to any other type of combination or isolated syllables such as A alone, B alone, BA combination, AA combination, AAA combination, etc.

In toto, to have a biophysically plausible neural network, we need our model to have the following features:

1- The CSN should generate suprathreshold firing responses to A then B stimuli, but not to A alone, B alone or B then A.
2- The CSN should start spiking at a time ranging from the onset to the offset of syllable B presentation.
3- The CSN should fire even when B is delayed from A by a certain intersyllable interval.

As we will see next, we incorporate all these biophysical features in our networks and derive a realistic explanation of this important property that HVC neurons exhibit.

B. Computational Analysis

First, we model single HVC_X, HVC_{INT} and HVC_{RA} neurons. These three types of neurons have different electrophysiological and morphological properties stated earlier. We will use the pharmacologically identified ionic currents to model our conductance-based neural networks (Daou, Ross et al. 2013). Our models are all Hodgkin and Huxley based. Equations 1-3 represent the voltage membrane dependence on the relative ionic

currents for HVC_X, HVC_{INT} and HVC_{RA} respectively, as developed by Daou, Ross et al 2013.

$$C_m \frac{dV_x}{dt} = -I_L - I_K - I_H - I_{Na} - I_{Ca-L} - I_{Ca-T} - I_{SK} + I_{app} \quad (1)$$

$$C_m \frac{dV_{INT}}{dt} = -I_L - I_K - I_H - I_{Na} - I_{Ca-L} - I_{Ca-T} + I_{app} \quad (2)$$

$$C_m \frac{dV_{RA}}{dt} = -I_L - I_K - I_A - I_{Na} - I_{Ca-L} - I_{SK} + I_{app} \quad (3)$$

Where C_m is the membrane capacitance, V_x, V_{INT} and V_{RA} are the membrane potential for HVC_X, HVC_{INT} and HVC_{RA} respectively, I_L is the leak current, I_{app} is the applied current and the rest are ionic currents modeled using Hodgkin and Huxley formalism as well. For all of the currents modeled above, we have:

$$I = g\, m^x\, h^y\, (V - E)$$

Where g is the maximal conductance, x is the number of gate activation, y is the number of gate inactivation, E is reversal potential of the specific ion and V is the membrane potential.

The rate of change of each activation/inactivation variable x follows the first order differential equation:

$$\frac{dx}{dt} = \frac{x_\infty - x}{\tau_x} \text{ where } x = n, h, e$$

With τ_x the time constant of x, x_∞ its steady state value, and x being one of activation/inactivation variables x=n,h. In the following equations, we define θ_x to be the half-activation voltage for the gating variable x and σ_x to be its slope factor for x=n,m,s.

Potassium current I_K:

$$I_K = g_K\, n^4\, (V - V_K)$$

$$n_\infty = \frac{1}{1 + \exp\left(\frac{V - \theta_n}{\sigma_n}\right)}$$

$$\tau_n = \frac{10}{\cosh\left(\frac{V - \theta_n}{2\,\sigma_n}\right)}$$

Sodium current I_{Na}:

$$I_{Na} = g_{Na} m_\infty^3(V) h\, (V - V_{Na})$$

$$m_\infty = \frac{1}{1 + \exp\left(\frac{V - \theta_m}{\sigma_m}\right)}$$

$$\alpha_h = 0.128 \exp\left(\frac{V + 50}{80}\right)$$

$$\beta_h = \frac{4}{1 + \exp\left(\frac{-(V + 27)}{5}\right)}$$

$$h = \frac{\alpha_h}{\alpha_h + \beta_h}$$

L-Type Calcium current I_{CaL}:

$$I_{CaL} = g_{CaL} V s_\infty^2(V)\left(\frac{Ca_{ex}}{1 - \exp\left(\frac{2FV}{RT}\right)}\right)$$

$$s_\infty = \frac{1}{1 + \exp\left(\frac{V - \theta_s}{\sigma_s}\right)}$$

T-Type Calcium current I_{CaT}:

$$I_{CaL} = g_{CaT} V [a_T]_{\infty}^{3}(V)[b_T]_{\infty}^{3}(r_T^A)\left(\frac{Ca_{ex}}{1 - \exp\left(\frac{2FV}{RT}\right)}\right)$$

$$a_{T\infty}(V) = \frac{1}{1 + \exp\left(\frac{v - \theta_{a_T}}{\sigma_{a_T}}\right)}$$

$$b_{T\infty}(r_T) = \frac{1}{1 + \exp\left(\frac{r_T - \theta_b}{\sigma_b}\right)} - \frac{1}{1 + \exp\left(\frac{-\theta_b}{\sigma_b}\right)}$$

Where the slowly operating gating variable r_T is governed by

$$\frac{dr_T}{dt} = \frac{r_{T\infty}(V) - r_T}{\tau_{r_T}(V)}$$

$$r_{T\infty}(V) = \frac{1}{1 + \exp\left(\frac{v - \theta_{r_T}}{\sigma_{r_T}}\right)}$$

$$\tau_{r_T}(V) = \tau_{r_0} + \frac{\tau_{r_1}}{1 + \exp\left(\frac{v - \theta_{r_T}}{\sigma_{r_T}}\right)}$$

Where $\frac{F}{RT}$ is the thermal voltage, *T* is the temperature of the bathing solution (25°C or 298 K), *R* is the gas constant, and *F* is Faraday's constant. Ca_{ex} is the external Ca^{2+} concentration.

Calcium dependent K^+ current:

$$I_{SK} = g_{CaL} k_{\infty}([Ca^{2+}]_i)(V - V_K)$$

$$k_{\infty}([Ca^{2+}]_i) = \frac{[Ca^{2+}]_i^2}{[Ca^{2+}]_i^2 + k_s^2}$$

$$\frac{d[Ca^{2+}]_i}{dt} = -f\{\in (I_{CaL} + I_{CaT}) + k_{Ca}([Ca^{2+}]_i - b_{Ca})$$

Where the constant f represents the fraction of free to total cytosolic Ca^{2+}, $\in$ combines the effects of buffers, cell volume and molar charge of calcium, k_{Ca} represents the calcium pump rate and b_{Ca} represents the basal level of Ca^{2+}.

Hyperpolarization-activated inward current I_H:

$$I_H = g_H[k_r r_f + (1 - k_r)r_s](V - V_H)$$

$$\frac{dr_f}{dt} = \frac{r_{f_\infty}(V) - r_f}{\tau_{r_f}(V)}$$

$$r_{f_\infty}(V) = \frac{1}{1 + \exp\left(\frac{v - \theta_{r_f}}{\sigma_{r_f}}\right)}$$

$$\tau_{r_f}(V) = \frac{p_{r_f}}{\frac{-7.4(V + 70)}{\exp\left(\frac{V + 70}{-0.8}\right) - 1} + 65\exp\left(\frac{V + 56}{-23}\right)}$$

$$\frac{dr_s}{dt} = \frac{r_{s_\infty}(V) - r_s}{\tau_{r_s}(V)}$$

$$r_{s_\infty}(V) = \frac{1}{1 + \exp\left(\frac{v - \theta_{r_s}}{\sigma_{r_s}}\right)}$$

The A-type Potassium current I_A:

$$I_A = g_A a_\infty(V) e(V - V_K)$$

$$a_\infty = \frac{1}{1 + \exp\left(\frac{V - \theta_a}{\sigma_a}\right)}$$

$$e_\infty = \frac{1}{1 + \exp\left(\frac{V - \theta_e}{\sigma_e}\right)}$$

The leak current I_L:

$$I_L = g_L(V - V_K)$$

The constant parameters of the previous equations are shown in Table 2 below.

Table 2: Constant Parameters Values For Ionic Currents

Parameter	Value	Parameter	Value	Parameter	Value
V_{Na}	50	V_K	-90	V_L	-70
V_H	-30	V_{Ca}	80	τ_n	10
τ_h	1	τ_{rf}	26.7	Ca_{ex}	2.5
θ_m	-35	θ_n	-30	σ_m	-5
σ_n	-5	θ_s	-20	σ_s	-0.05
θ_{aT}	-65	σ_{aT}	-7.8	θ_b	0.4
σ_b	-0.1	θ_{rT}	-67	σ_{rT}	2
θ_{rf}	-105	σ_{rf}	5	θ_{rs}	-105
σ_{rs}	25	C_x	100	C_{INT}	75
F	0.1	$\in$	0.0015	K_{Ca}	0.3
τ_e	20	σ_e	5	θ_e	-60
σ_a	-10	θ_a	-20		

To model the network dynamics, synaptic connections were integrated to individual neurons. The pharmacological nature of the synaptic currents (AMPA/NMDA/GABA/…) were based on data collected with dual whole-cell recordings in brain slices (Mooney and Prather 2005). Therefore, in addition to the currents presented in equations 1 and 2, each neuron receives a particular set of synaptic currents as described below.

In the set of equations shown below, g_X is the maximal conductance of X current, tuned for each neuron and each circuit differently, a_r and a_d are respectively constants characterizing the rise and decay rates of synaptic conductance, [T] is the concentration of neurotransmitters released by the presynaptic neuron, V_{pre} is the membrane potential of the presynaptic neuron, T_{max} is the maximal value of neurotransmitters, K_p is a constant. Typical values for the parameters above are shown in Table 3.

For neurons receiving AMPA and NMDA synapses, we add I_{AMPA} and I_{NMDA} as such:

$$I_{AMPA} = g_{AMPA} s_{AMPA} (V - V_{AMPA})$$

$$\frac{ds_{AMPA}}{dt} = a_{rAMPA}[T](1 - s_{AMPA}) - a_{dAMPA} s_{AMPA}$$

$$T(V_{pre}) = \frac{T_{max}}{1 + \exp\left(\frac{-(V_{pre} - V_T)}{K_p}\right)}$$

$$I_{NMDA} = g_{NMDA} s_{NMDA} B(V)(V - V_{NMDA})$$

$$\frac{ds_{NMDA}}{dt} = a_{rNMDA}[T](1 - s_{NMDA}) - a_{dNMDA} s_{NMDA}$$

$$T(V_{pre}) = \frac{T_{max}}{1 + \exp\left(\frac{-(V_{pre} - V_T)}{K_p}\right)}$$

$$B(V) = \frac{1}{1 + \exp(-0.062V)\frac{[Mg^{2+}]}{3.75}}$$

For neurons with $GABA_A$ and $GABA_B$ connections, we add I_{GA} and I_{GB} currents as such:

$$I_{GA} = g_{GA} s_{GA} (V - V_{GA})$$

$$\frac{ds_{GA}}{dt} = a_{rGA}[T](1 - s_{GA}) - a_{dGA}s_{GA}$$

$$T(V_{pre}) = \frac{T_{max}}{1 + \exp\left(\frac{-(V_{pre} - V_T)}{K_p}\right)}$$

$$I_{GB} = g_{GB}\frac{s^n}{k_d + s^n}(V - E_K)$$

$$\frac{ds}{dt} = k_3 r - k_4 s$$

$$\frac{dr}{dt} = a_r[T](1 - r) - b_r r$$

Table 3: Constant Parameters Values For Synaptic Currents

PARAMETER	VALUE
$\mathbf{V_{AMPA}}$	**0 mV**
$\mathbf{a_{rAMPA}}$	**1.1 $mM^{-1}ms^{-1}$**
$\mathbf{a_{dAMPA}}$	**0.19 ms^{-1}**
$\mathbf{V_{NMDA}}$	**0 mV**
$\mathbf{a_{rNMDA}}$	**0.072 $mM^{-1}ms^{-1}$**
$\mathbf{a_{dNMDA}}$	**0.0066 ms^{-1}**
$\mathbf{V_{GA}}$	**-70 mV**
$\mathbf{a_{rGA}}$	**5 $mM^{-1}ms^{-1}$**
$\mathbf{a_{dGA}}$	**0.18 ms^{-1}**
$\mathbf{a_{rGB}}$	**0.09 $mM^{-1}ms^{-1}$**
$\mathbf{a_{dGB}}$	**0.0012 ms^{-1}**

n	**4**
k_d	**100**
k_3	**0.18 ms^{-1}**
k_4	**0.034 ms^{-1}**
k_p	**5 mV**
T_{max}	**1 mM**
V_T	**2 mV**

In each circuit model developed, two excitatory selective neurons of HVC_X type are added. One is selective to the first syllable A, and another to the second syllable B. To indicate the presentation of one of the syllables, we simulate the model such that A-selective or B-selective neuron fires. To present syllable A, a DC current is applied to A-selective neuron for 150 msec (roughly the duration of a syllable). The same process is undertaken for the presentation of syllable B. The current applied I_{app} in equations 1 and 2 is therefore zero for all neurons except in A-selective and B-selective neurons during the presentation of their corresponding syllables.

After the full development of functional networks, we investigated the effects of temperature variations in our networks in order to check for the networks' robustness and their realistic changes. While we know that higher temperatures are associated with higher neuronal excitability, it's not known whether challenging the HVC network by varying the temperature would break down their robustness and thereby eliminate the combination-sensitivity property that some neurons exhibit.

The temperature factor, knowing as the Q factor, is defined as the quantitative change in a physiological property for a 10^0 change in temperature as can be inferred from Equation (4) below.

$$\frac{P_T}{P_{Tref}} = Q^{\frac{T-Tref}{10}} \quad (4)$$

Where P_T is the property value at the current temperature T and P_{Tref} is the property value at the reference temperature T_{ref}.

The Q factor is integrated in the modelling equations presented above by simply defining a value for the Q factor and multiplying all activation/inactivation parameters with the factor on the right side of Equation (4) above. This is shown in Equation (5).

$$x = f(x)\, Q^{\frac{T-Tref}{10}} \qquad x = n, m. h, s, a, e, a_T, b_T, r_T, k, r_f, r_s$$

where f(x) represents the functions defined previously in the section for each of the variables.

We will note the variation in behavior when T increases for the original duration of syllable presentation of 150msec as well as for a shorter duration of 100msec.

Simulations of these model neurons are being performed using custom built MATLAB (MathWorks) code. Our goal is not to isolate the best network architecture that explains the combination sensitivity property, but to explore and compare different possible realistic scenarios in which the different types of HVC neurons can interact to produce this behavior.

CHAPTER IV

RESULTS

We have created five different wiring diagrams that represent biophysically plausible scenarios leading up to the combination-sensitivity property. In all of the networks presented in this section, neurons have been modeled using pharmacologically identified ionic currents (Daou, Ross et al. 2013) and they are connected via previously identified synaptic currents (Mooney and Prather 2005) (see Methodology for further details). In this paper, we focus on selectivity to a couple of signals arriving in a certain temporal order. For songbirds, this signal would be represented by a syllable. We use the notation 'syllable A' for the signal that should be presented first and 'syllable B' for the signal that should follow. In order to assess the output of a model, we test it under four different conditions: 1- When syllable A is presented alone, 2- When syllable B is presented alone, 3- When syllable A precedes syllable B and 4- When syllable B precedes syllable A. The model satisfies combination-sensitivity when the combination sensitive neuron (CSN) fires in the third case scenario only, i.e. when syllable A precedes syllable B. All circuitries include three auditory-selective HVC neurons essential for the functionality of the network: an A-selective neuron that elicits action potential burst when the syllable A is presented alone, a B-selective neuron that fires a response when syllable B is presented alone and an AB-selective neuron (the CSN) which should fire - as previously indicated - in the only case where syllable B follows syllable A. Each neuron in our microcircuit designs is modeled as a mean field neuron, meaning that it is representative of a neural population. We envision the HVC to be composed of many copies of such microcircuits that are associated with combination-sensitivity with roughly

synchronized activity (Fee, Kozhevnikov et al. 2004). Moreover, HVC neurons receive afferent projections from several extrinsic forebrain and brainstem regions (Nottebohm, Paton et al. 1982, Foster, Mehta et al. 1997, Cardin and Schmidt 2004). Since little is known about the firing pattern of this input and it modulates the activity of each class of HVC neuron, we treat it as a DC current which is on during playback of the bird's own song and applied to the three HVC neuronal populations.

Since it's largely unknown how HVC neurons perceive auditory information and respond selectively to auditory stimuli, and since our main goal here is to explain the combination-sensitivity mechanism at the level of the HVC network and not explain the nature of the auditory neural code (although the two are interconnected), we drove selectivity of any single particular syllable with a DC current. In other words, whenever we want a selective HVC neuron to respond to a syllable, we inject a DC-current into that neuron, with a duration that's on average similar to the syllable duration, driving the corresponding neuron for the entirety of current application. The goal here is to generate spikes in the syllable-selective neuron to kick start the network. Later we present input to the network from actual recorded bird songs (syllables) filtered through spectral temporal receptive fields, similar to what's been done before (Drew and Abbott 2002). To that end, both A-selective and B-selective neuron will be stimulated with a DC current for 150 msec which represents an average syllable duration.

In many network models presented in this section, neurons might have more than one synaptic input at the same time. This concept of summation of signals at the level of synapses has been previously investigated for a variety of purposes and in many types of species. It was originally thought that two different synaptic input arriving to one postsynaptic neuron will have a decreased joint effect on the neuron if they have taken

the same dendritic path and an increased joint effect if the dendrites are different. Nevertheless, this idea has been refuted by experimental studies that prove the summation of synaptic input to the neuron regardless of the source (Cash and Yuste 1998, Wessel, Kristan et al. 1999). In Powers and Binder 2000 study on cat motor neurons, the authors show that adding different current inputs onto the same neuron results in the neuron firing action potentials at a higher frequency, which indicates that the different currents' effects on the neuron were summed and the signal was amplified every time a new depolarizing current was added. The authors also note a relatively opposite behavior when a current of an opposite signal is added to the input of the neuron, validating the idea of synaptic effects summation further (Powers and Binder 2000). A later study proved that the injection of a current to a neuron that is receiving an independent synaptic current at the same time will also result in an increase in the firing rate of the neuron (Prather, Powers et al. 2001). These results are very similar to other studies that have on the effect of two or more synaptic inputs to a neuron for cats (Hyngstrom, Johnson et al. 2008) and for other species such as the leech (Wessel, Kristan et al. 1999) and the rat (Cash and Yuste 1998, Margulis and Tang 1998, Léger, Stern et al. 2005). And although the true nature of synaptic summation is still being investigated, we can try to infer the behavior of the neurons to more than one synaptic current when there exists knowledge of their physiological properties and the nature of their synaptic connections, which is the case in our work here.

We divide the five architectural scenarios we developed to two categories based on the classes of HVC neurons they integrate: three circuit models will include excitatory HVC_X neurons and inhibitory HVC_{INT} neurons solely and two other circuits will additionally include excitatory HVC_{RA} neurons. To study the robustness of the networks,

and to mimic a more realistic firing of HVC neurons, we "heated up" the network by modifying the Q10 factor, which changes the channel conductances as a function of temperature. In short, the Q10 factor is the ratio between the rate of a certain biological process (in our case, neuronal firing which depends on ion channel dynamics) at two temperatures separated by 10 °C, and it's a direct measure of the degree to which the neuronal firing and the network dynamics depend on temperature (O'Leary and Marder 2016). The temperature factor Q was implemented in all of our network models. Furthermore, we added a delay factor allowing the CSN to elicit action potential burst even when the syllables' presentations are separated by a long interval of time, called the intersyllable interval, as seen experimentally (Margoliash 1983, Margoliash and Fortune 1992).

A. Circuit network including HVC_X and HVC_{INT} neurons:

1. Circuit 1: Rebound burst of HVC_X neuron:

The architecture of the first model consists of HVC_X and HVC_{INT} neurons connected to each other in a microcircuit as shown in Fig. 8. There are "A", "B" and "AB" labels in Fig. 8, representing A-selective, B-selective and AB-selective neurons, respectively. For example, an A-selective neuron is an HVC neuron (an X-projecting HVC_X neuron) that fires only when syllable A is presented, and remains silent otherwise. In this, and subsequent networks, the propagation of activity starts from either the A-selective or the B-selective neuron depending on which syllable is presented first.

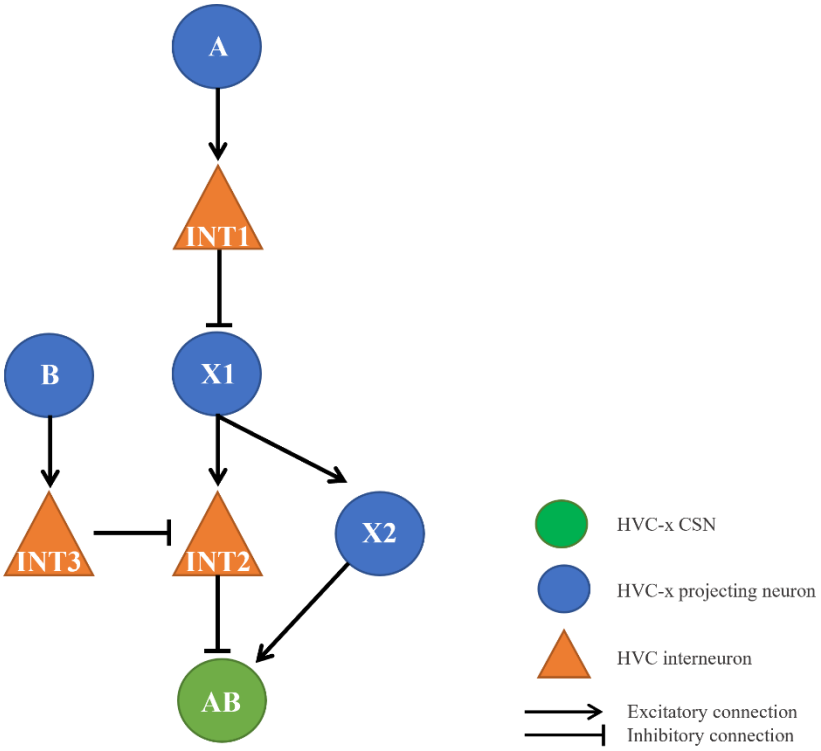

Figure 8: Network model 1 showing all different excitatory and inhibitory synaptic connections between projection HVC_X neurons (blue circles) and inhibitory HVC_{INT} neurons (orange triangles) and the CSN neuron (green circle). Selective neurons are named according to what they are selective to. "A" for A-selective neuron that fires when syllable A is presented alone, "B" for the B-selective neuron that fires when syllable B is presented alone and "AB" for the CSN neuron that fires when A is presented followed by B.

a. Syllable A presentation:

When syllable A is presented alone (i.e. a DC current pulse injected onto the A-selective projecting neuron), the neuron fires a burst of action potentials mimicking the response to the presentation of syllable A (Fig. 9A)As a result of this firing, interneuron HVC_{INT} (INT_1) fires due to excitatory AMPA and NMDA coupling from the A-selective neuron (Fig. 9B). INT_1 will in its turn send an inhibitory signal down its GABAergic connections to the HVC_X neuron X_1. These three events (A-selective firing, then INT_1 firing, followed by X_1 inhibited, all occur at the same instance of time, due to fast excitatory and inhibitory signaling, with a very little delay). When the A-selective neuron finishes its burst of action potentials, INT_1 will stop firing because its excitatory drive is

over and as a result the X_1 neuron will be able to escape the inhibition of INT_1. The inhibition that INT_1 exerts on X_1 activates the hyperpolarization activated inward current (I_h) as well as the T-type Ca^{2+} current (I_{CaT}) which are expressed in all HVC_X neurons and which are included in the model (Daou, Ross et al. 2013). This will generate a postinhibitory rebound burst in X_1 (Fig. 9C) modulated by both synaptic (GABA) as well as intrinsic (I_h + I_{CaT} ionic currents) mechanisms. The rebound burst that X_1 generates will send an excitatory signal onto both INT_2 and X_2 neurons in the network at the same time, eliciting excitatory responses in both neurons (Fig. 9D). As a result of this excitation, the combination sensitive neuron (AB-selective) will then receive an excitatory input from X_2 and an inhibitory input from INT_2 at the same time (Fig. 9D). The two opposite signals (one excitatory from X_2 and another inhibitory from INT_2) will cancel out at the CSN synapses and therefore the CSN will remain silent (Fig. 9D). This is consistent with what's seen experimentally where the playback of one (first) syllable alone does not elicit a response in the CSN neuron (Margoliash 1983, Lewicki and Konishi 1995, Lewicki and Arthur 1996). This cancelation of excitatory and inhibitory synapses is a key feature in most of our network models.

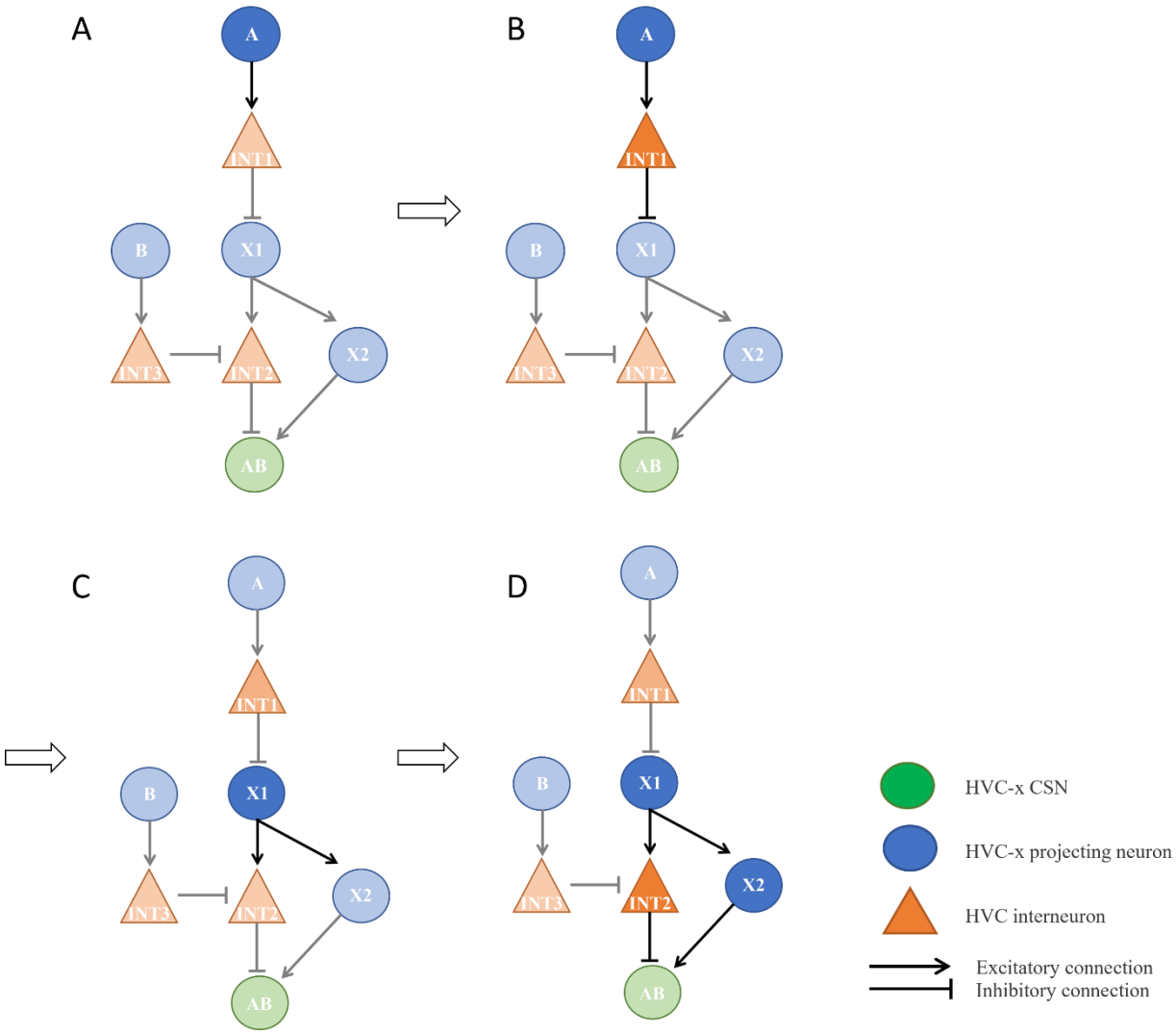

Figure 9: Syllable A presentation in network architecture 1. HVC_X and HVC_{INT} neurons are color coded as shown in Fig. 8. The diagram represents the flow in time of the corresponding firing neurons when syllable A is presented solely. Arrows represent the flow in time. Dark colors represent excited neurons that are currently firing spikes as well as operating synaptic connections and light colors represent silent neurons and resting synaptic connections (see text).

b. Syllable B presentation:

If syllable B is played back solely (i.e. applying a positive DC-current pulse onto the B-selective projection neuron), the neuron fires a burst of action potentials, sending depolarizing signals down to INT_3 because of the excitatory AMPA and NMDA coupling between them (Fig. 10A). The firing of INT_3 will then generate an inhibitory response in INT_2 due to GABAergic inhibitory coupling. The signal therefore will die out with INT_3

neuron and no other neurons in the circuit will fire including the CSN (Fig. 10B), rendering the presentation of syllable B alone ineffective towards the firing of the CSN neuron. This represents another feature of the CSN as recorded *in-vivo*, where the CSN will stay silent during the presentation of the second syllable alone (Margoliash 1983, Lewicki and Konishi 1995, Lewicki and Arthur 1996).

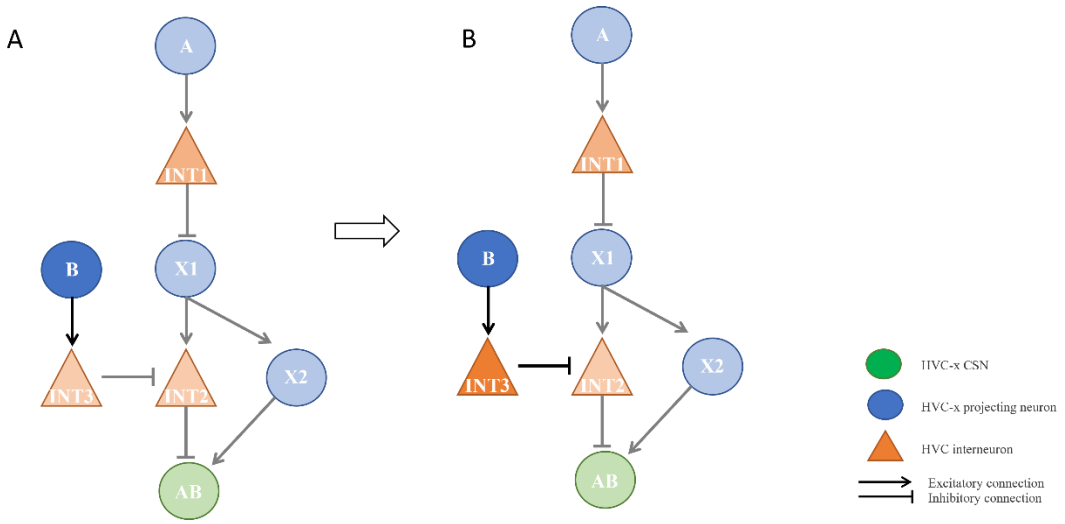

Figure 10: Syllable B presentation in network architecture 1. The diagram illustrates the flow of activity when syllable B is presented solely. The AB-selective neuron (CSN) remains silent as INT_3 inhibits INT_2 rendering the pathway from B effectively silent.

The CSN neuron is supposed to fire only when syllable A is followed by syllable B (sometimes with a delay in between both syllable presentations, which we will address later). When both syllables are presented consecutively, the CSN's response depends on which syllable was presented first. If syllable B was presented before A, the signal will die as soon as the B-selective neuron stops firing (Fig. 10), and in that case, the presentation of syllable A after B will have the same effect on the network as when syllable A is presented alone (Fig. 9). Only when the right order of syllables is presented, this network architecture is able to excite the AB neuron as described next.

c. Syllable A followed by syllable B presentation:

The first few steps of this scenario are similar to the case when syllable A is presented alone, that is, A-selective neuron fires (Fig. 11A), exciting INT_1 (Fig. 11B), the latter inhibiting X_1 which then generates a rebound burst (Fig. 11C). Now, the firing of X_1 is coincided with the presentation of syllable B, because X_1 neuron fires only when the A-selective neuron finishes its burst, which signifies the end of the presentation of syllable A. Therefore, the B-selective neuron is now active at the same time the X_1 neuron is generating its rebound (Fig. 11C). The simultaneous firing of X_1 and B-selective neurons will generate excitatory responses in INT_3 (from B-selective) and X_2 (from X_1), and supposedly in INT_2 because of the excitatory coupling from X_1 (Fig. 11D). However, the burst in INT_2 does not happen because this interneuron is not able now to escape the simultaneous inhibition that it receives at the same moment in time it's about to fire from INT_3. In other words, the network is structured such that the inhibition INT_2 receives from INT_3 is greater than the excitation it receives from X_1 rendering INT_2's activity silent when both excitation and inhibition arrive simultaneously at its synapses. This is important, because now X_2 neuron which just fired is able to generate a response in the CSN neuron (AB-selective). In other words, out of the two opposite synaptic connections arriving at the CSN, the excitatory signal X_2 will now be the only signal that the CSN is receiving (unlike what we saw earlier in the case of syllable A presented alone where we saw how excitation and inhibition canceled each other at the CSN sites). The CSN will then be depolarized and elicit a series of action potentials as a result of one and only one scenario: syllable A preceded syllable B in presentation (Fig. 11E).

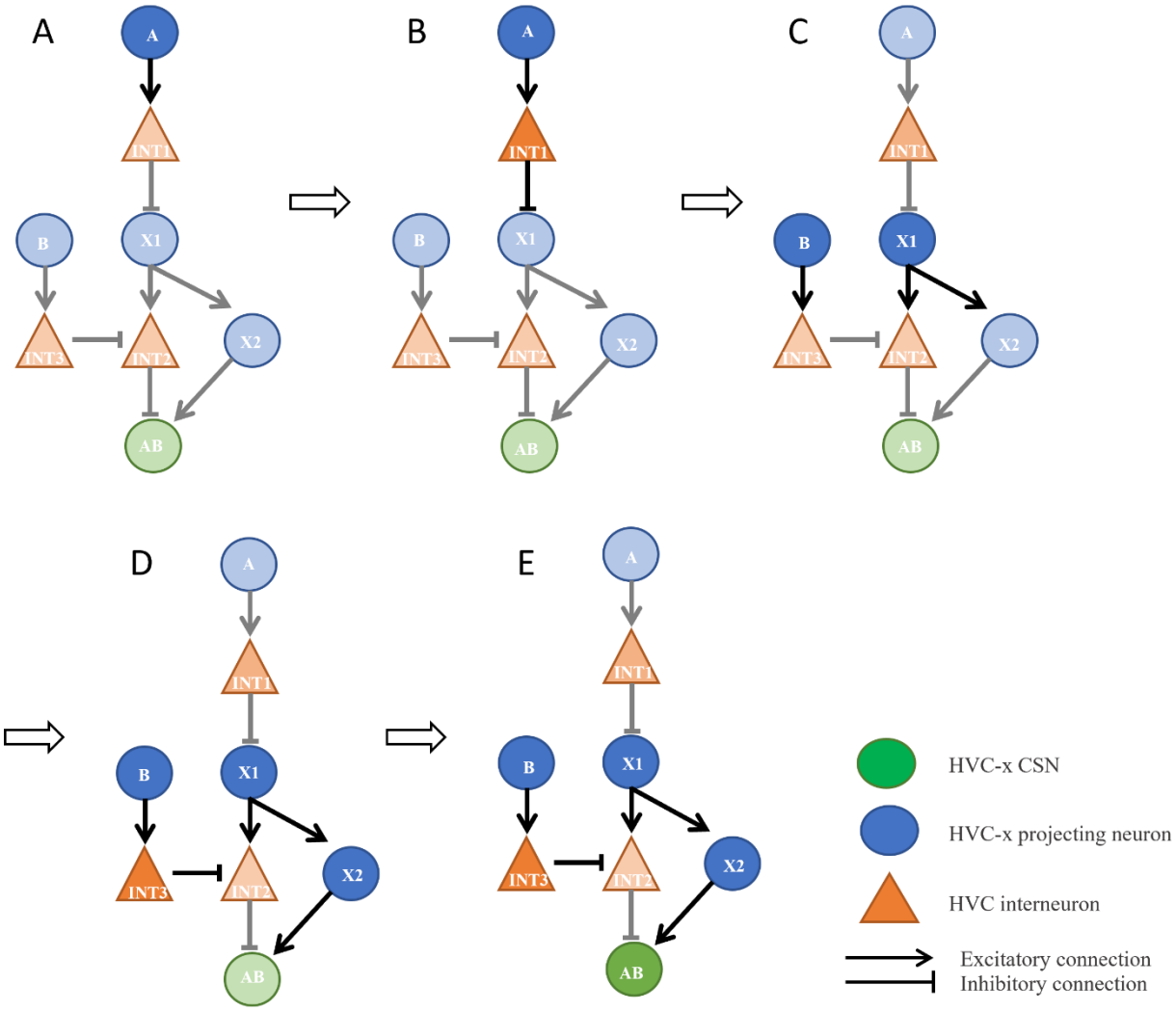

Figure 11: Network model 1 consisting of the appropriate HVCX and HVCINT neurons shown in Fig. 8. The diagram represents the flow in time of firing neurons when syllable A presentation directly precedes syllable B presentation. Arrows represent the flow in time. Dark colors represent excited neurons that are currently firing spikes as well as operating synaptic connections and light colors represent silent neurons and resting synaptic connections (see text).

The firing patterns of syllable-selective neurons that this network exhibits are presented in Fig 12. When syllable A is presented alone (Fig. 12A), syllable B presented alone (Fig. 12B), or syllable B preceding B (Fig. 12C), the AB-selective neuron is silent as described before. Only when the right order of syllables are presented (A then B) that the CSN is able to generate a response (Fig. 12D).

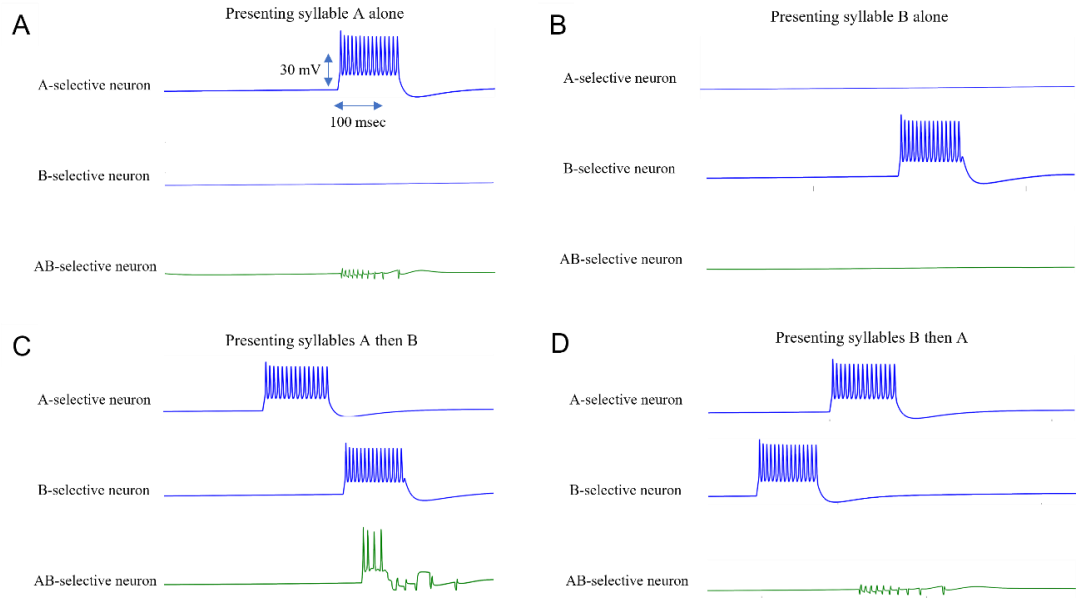

Figure 12: Firing patterns of the syllable-selective neurons in response to different syllable stimuli for network model 1, when presenting syllable A alone (A), presenting syllable B alone (B), presenting syllable A followed by B (C), presenting B followed by A (*D*). The AB-selective neuron only fires when A is followed by B.

The activity patterns that all neurons in this network exhibits are illustrated in the raster plot of Fig. 13. The A-selective projection neuron fires first in the series exciting INT_1 which spikes continuously (notice frequencies shown in figure) inhibiting X_1. The degree of inhibition from INT_1 to X_1 dictates the speed and the strength of generating a postinhibitory rebound burst. This is controlled by the maximal GABAergic synaptic conductances (see Methods). B-selective neuron fires next (simultaneously with X_1 exciting INT_3. This excitation stops the firing of INT_2 due to the strong inhibitory coupling onto INT_2. As shown in Fig. 13, INT_2 is eventually able to escape this inhibition and fires a response. The latency and degree of this response is magnified by two factors: 1) the postinhibitory effect it can generate from the inhibition of INT_3 due to the expression of T-type Ca^{2+} and H- channels, and 2) the excitation from X_1. Therefore, there is a balance of excitation and inhibition happening at the level of INT_2 such that one could win over the other depending on the strength of the synaptic and intrinsic

conductances. What is needed to make this network work is to have inhibition stronger than excitation such that INT_2 does not fire at the same time as X_2 neuron (Fig. 13).

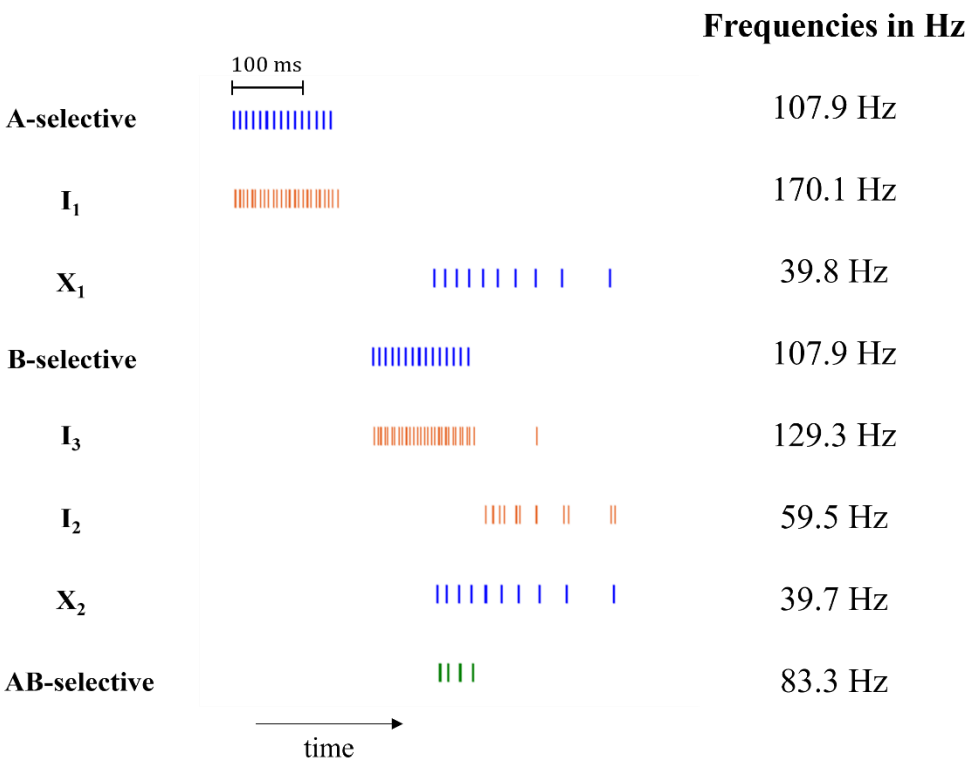

Figure 13: Raster plot depicting the firing activity for network model 1 and showing the neurons' responses in time. Each tick mark in a row represents an action potential for the corresponding neuron in that row. The spikes are arranged exactly as they occur in time. Blue spikes represent HVC_X neurons' spikes and orange spikes represent HVC_{INT} neurons' spikes. The overlap in firing between I_3 and X_2 causes the AB-selective neuron to fire (see text).

2. Circuit 2: Inhibitory chain of HVC_{INT} neuron:

The second network architecture is mainly based on a chain of inhibitory and excitatory neurons involving interneurons and X-projecting neurons. This network utilizes excitatory and inhibitory loops to encode temporal information over prolonged periods of time, as we will describe below (Fig. 14). Once again, the network configuration will not allow the firing of the CSN unless A is followed by B. For example, the presentation of syllable A alone induces the spiking of its postsynaptic neuron INT_1 twice that occurs at two different times: the first is through its direct synaptic

AMPA/NMDA connection and the second one is through a tri-synaptic pathway where the A-selective neuron excites interneuron INT_3 which will in its turn inhibit projecting neuron X_4 and, when inhibition is strong enough, X_4 will exhibit a rebound burst due to the activation of its I_h and I_{CaT} currents, ultimately exciting INT_1. The presence of multiple synapses in this second pathway is to integrate information over time as such: As long as syllable A is being presented, the A-selective neuron is firing and therefore INT_1 is firing inhibiting the pathway that leads to AB-selective neuron. When syllable A is over, both A-selective and INT_1 end their spike trains, but INT_1 will readily continue its spiking due to the excitation it receives from the second pathway involving INT_3 and X_4. The exact time this excitation reaches INT_1's synapses depends on several factors including 1) the strength of excitation from A-selective to INT_3 (weaker excitation will delay signal transmission), 2) strength of inhibition from INT_3 to X_4 (stronger inhibition will generate strong X_4 rebounds and therefore faster signal transmission to INT_1, 3) strength of excitation from X_4 to INT_1 and 4) strength of T-type Ca^{2+} and H-currents conductances in X_4 (which controls the strength of the rebound burst). , Information coming from both pathways will ensure that INT_1 is always inhibiting neuron INT_2, thereby fading the signal away. On the other hand, presentation of syllable B alone will activate two different paths, both of which are tri-synaptic: the first one is through the excitation of X_2, exciting in its turn X_3, which eventually activates X_3 , the last neuron in this chain that will turn on the CSN. Nevertheless, we don't want the CSN to be activated when syllable B is presented alone, and here comes the role of the second pathway from B to shut down the activity of the first (B-selective excites X_1 which excites INT_2 inhibiting AB-selective neuron). The CSN will then be receiving both excitatory and inhibitory signals coming from both pathways, and thereby will remain silent when syllable B is presented alone. However,

when syllable A presentation is followed by syllable B (A-selective neuron firing followed by B-selective neuron firing), the rebound burst that the X_4 neuron generates (via the second pathway from A-selective) activates INT_1 and this will occur at the same time with the activation of the B-selective neuron.. This means that neuron INT_2 will be inhibited at the same time when neurons X_1 and X_3 are spiking. This inhibition renders the first pathway from the B-selective neuron (through X_1) ineffective and therefore the second pathway (via X_2 and X_3) will not be stopped by INT_2 and therefore the CSN neuron will fire.

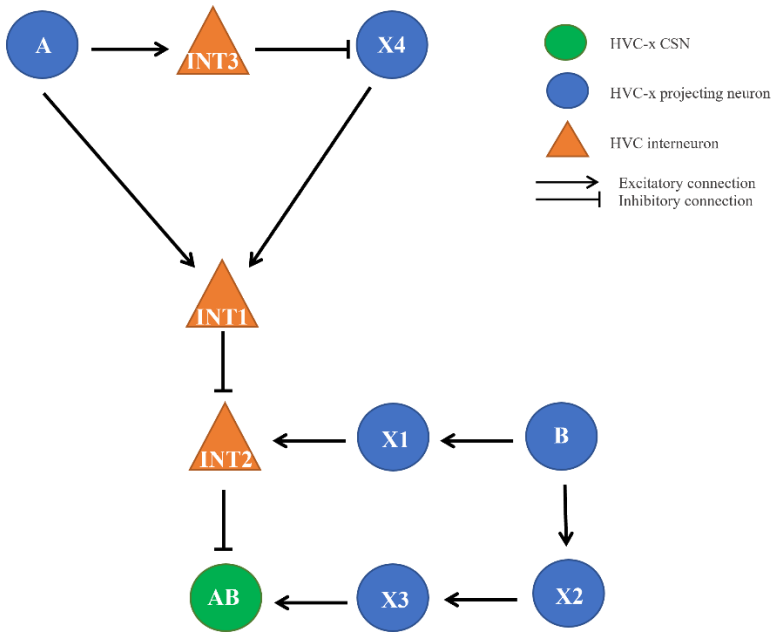

Figure 14: Network model 2 showing all different excitatory and inhibitory synaptic connections between HVCX neurons (blue circles) and HVCINT neurons (orange triangles) and the CSN neuron (green circle). Selective neurons are named according to what they are selective to. A for A-selective neuron, B for B-selective neuron and AB for AB-selective neuron.

The activity patterns that all neurons in this network exhibits are illustrated in the raster plot of Fig. 15. A-selective neuron fires and causes both interneurons INT_1 and INT_3 to fire at the same time. INT_3 will inhibit X_4 and we can see that X_4 exhibits a small rebound burst after the inhibition. It is also clear how X_4's rebound burst coincides with

the firing of B-selective neuron, an important feature of this network. While X_4 will cause the firing of INT_1 (notice the low frequency firing of INT_1 after syllable B is presented), B-selective will send excitatory signals to neurons X_1 and X_2 (notice the two neurons firing at the same time as B-selective neuron) and they in turn will cause the excitation of neurons X_3 and INT_2. However, INT_2 firing will not be continuous due to the inhibitory input that it is receiving from INT_1 (notice that when INT_1 is spiking, INT_2 is silent). When INT_2 is silent, AB-selective neuron will be allowed to fire action potential spikes because it is free from inhibition.

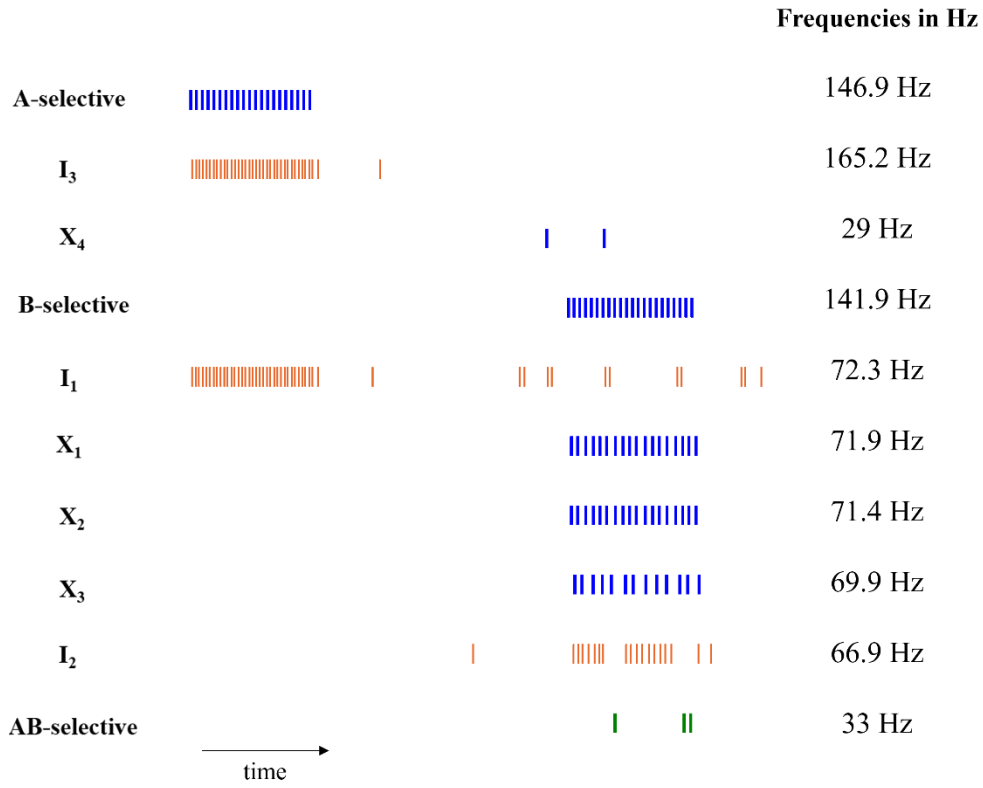

Figure 15: Raster plot depicting the firing activity for network 2 and showing the neurons' responses in time. Each tick mark in a row represents an action potential for the corresponding neuron in that row. The spikes are arranged exactly as they occur in time. Blue spikes represent HVC_X neurons' spikes and orange spikes represent HVC_{INT} neurons' spikes. The overlap in firing between I_1 and X_3 causes the AB-selective neuron to fire (see text).

3. Circuit 3: Double inhibition causes post-inhibitory rebound burst:

The third network architecture is based on the assumption that two different inhibitory signals arriving at the same HVC_X postsynaptic neuron consecutively and thereby keeping it hyperpolarized for a long period of time might result in the postsynaptic neuron's generation of a postinhibitory rebound burst even if each one of the two inhibitory signals alone is not enough to generate one. In this network, this is represented by the inhibitory neurons INT_1 and INT_2 both synapsing onto the same HVC_X neuron X_1 (Fig. 16). Similar to the previous networks explained, this CSN in this diagram will only fire if syllable A is presented and followed by syllable B. The presentation of syllable A to this network results in two different signaling pathways: on one hand, A-selective neuron sends an excitatory signal towards INT_1 and INT_1 fires a series of action potential spikes due to the AMPA/NMDA coupling to A-selective neuron. INT_1 then sends an inhibitory signal onto neuron X_1. This inhibition does not last long enough to cause a rebound burst in X_1 and once A-selective neuron and INT_1 go back to their resting membrane potential, the signal fades away. On the other hand, A-selective neuron sends an excitatory signal down to neuron INT_3 which in turn sends an inhibitory signal down its GABAergic synapse onto neuron X_4. After the presentation of syllable A is finished and the first couple of neurons stop firing, , X_4 escapes the inhibition and generates a rebound burst. As a result, INT_4 receives an excitatory signal due to the AMPA/NMDA coupling to X_4. INT_4 finally sends an inhibitory signal to the CSN and the CSN will become hyperpolarized. Presenting syllable B alone to this network induces the same signal trajectory as the former pathway explained for the presentation of syllable A, this time through the path of the excitation of B-selective neuron to imitate the presentation of syllable B → excitation of neuron INT_2 due to the excitatory coupling to the B-selective

neuron → inhibition of neuron X_1 by the interneuron INT_2 where the signal dies out. But if syllable A is presented followed by syllable B, neuron X_1 is inhibited first by INT_1 when syllable A is presented and, as soon as syllable A presentation is finished, X_1 will be inhibited again during the presentation of syllable B by INT_2. Therefore, the result is an inhibition onto X_1 for twice the duration in the cases of presenting A alone or B alone. X_1 will therefore be inhibited for a long period of time which will allow the activation of its I_H and I_{CaT} currents and hence a rebound burst generation after the termination of inhibition. This rebound burst will send an excitatory signal to the CSN and the CSN will consequently fire. If syllable B precedes syllable A, neuron X_1 will be inhibited for twice the previous duration which will cause a rebound burst. Ideally, this would in turn cause an excitatory response in the CSN. However, the burst of neuron X_1 will overlap in time with the burst of neuron X_4. The CSN will receive an excitatory input (from X_1) and an inhibitory input (from INT_4) at the same time which will stop the neuron from spiking.

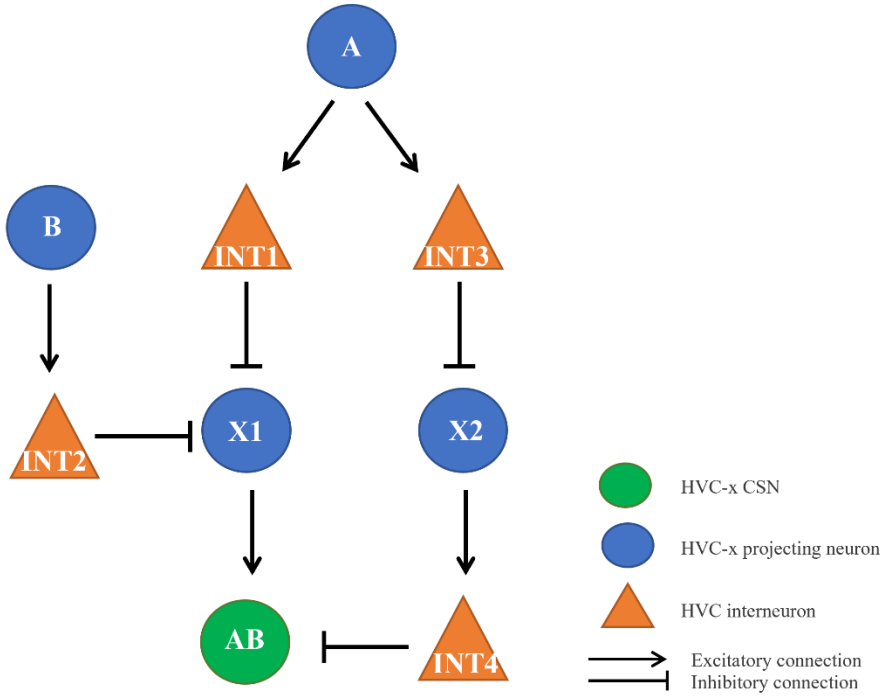

Figure 16: Network model 3 showing all different excitatory and inhibitory synaptic connections between HVCX neurons (blue circles) and HVCINT neurons (orange triangles) and the CSN neuron (green circle). Selective neurons are named according to what they are selective to. A for A-selective neuron, B for B-selective neuron and AB for AB-selective neuron.

In Fig. 17, we see the activity of all the neurons starting with A-selective neuron's action potential spikes which are accompanied with those of INT_1. The same pattern is present for B-selective neuron and INT_2. As can be seen in the raster plot, the spikes of INT_1 are now directly followed by those of INT_2 indicating that X_1 is being inhibited consecutively in time by these two neurons. The rebound burst of X_1 can be seen directly following the end of the INT_2 spikes. Notice that the inhibition from INT_4 to the CSN terminates prior in time than the rebound spiking of X_1 occurs. Therefore, the CSN is silent and is not receiving any other signal when X_1 sends an excitatory input to the CSN allowing it to fire as can be seen in Fig. 17.

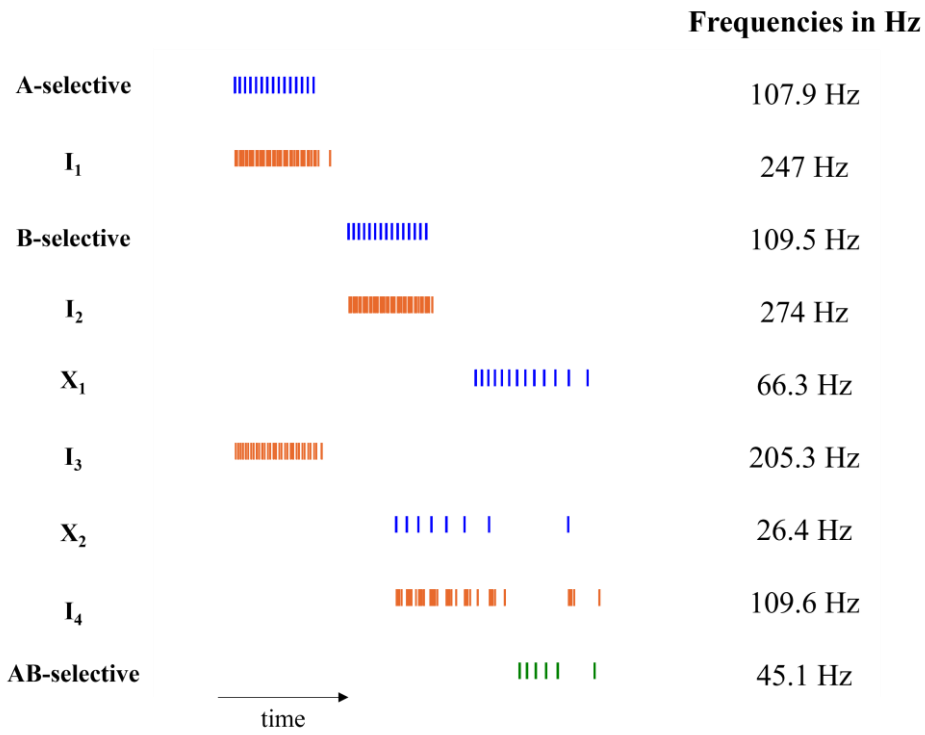

Figure 17: Raster plot depicting the firing activity for network 3 and showing the neurons' responses in time. Each tick mark in a row represents an action potential for the corresponding neuron in that row. The spikes are arranged exactly as they occur in time. Blue spikes represent HVC_X neurons' spikes and orange spikes represent HVC_{INT} neurons' spikes. The overlap of the rebound firing in X_1 and the silence of I_4 causes the CSN to fire (see text).

B. Circuit network including HVC_X, HVC_{RA} and HVC_{INT} neurons:

1. Circuit 4: Combination of rebound dPSP and minor excitatory signal:

The first circuit network that includes HVC_{RA} neuron is based on the fact that HVC_{RA} neurons are generally less excitable than HVC_X neurons and fire with a much lower frequency (Daou, Ross et al. 2013). Therefore, when an HVC_{RA} neuron synapses onto any other type of neuron, it is not necessarily true that an active HVC_{RA} neuron will definitely cause an excitatory response in the postsynaptic neuron. This diagram includes an HVC_{RA} neuron that synapses onto the CSN (Fig. 18). When syllable B is presented to the network, an input current will be applied to the B-selective neuron which will send an excitatory signal to the HVC_{RA} neuron RA. RA will then undergo an excitatory response due to the AMPA/NMDA coupling from B-selective neuron. This

excitatory response will have a much lower frequency than that of B-selective neuron to the difference in nature and ionic currents of these two classes of neurons. RA will therefore send a weak excitatory signal down to the CSN which will undergo small depolarizations dPSPs but will not fire any action potential burst. . When syllable A is presented alone, A-selective neuron will fire a series of action potential sending an excitatory signal to the interneuron INT which is coupled to the CSN. INT will fire and will inhibit the CSN for a certain duration after which the CSN will escape the inhibition and form small below threshold post-inhibitory depolarizations dPSPs. However, if syllable A is presented first and syllable B followed, then the latter dPSPs mentioned resulting from the post-inhibitory rebound will coincide will the former dPSPs mentioned caused by the low frequency excitation from neuron RA. When this interference in depolarizing signals happens, the CSN's potential will exceed the threshold and the CSN generates a response of action potential spikes (Fig. 19).

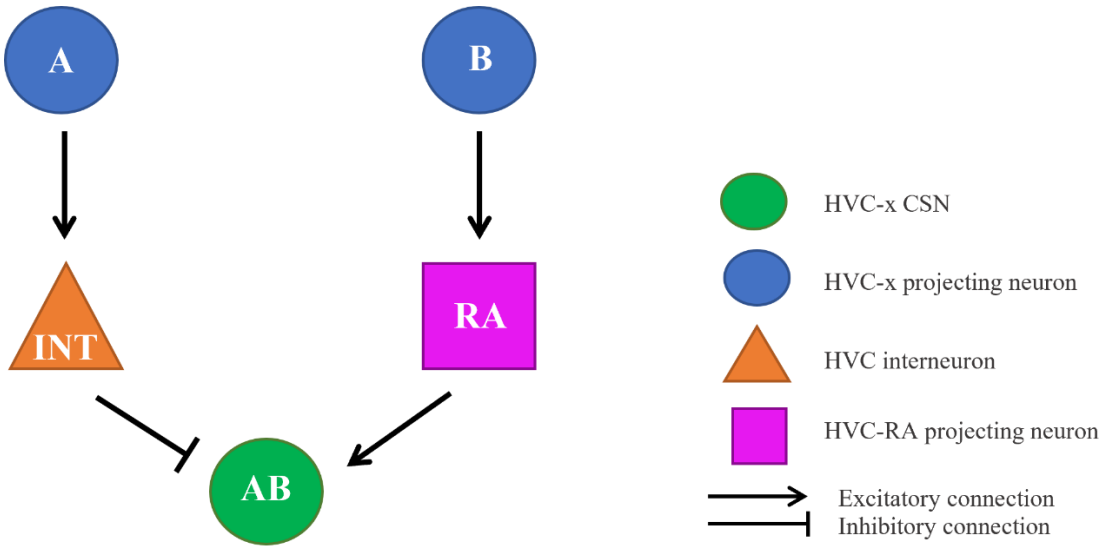

Figure 18: Network model 4 showing all different excitatory and inhibitory synaptic connections between HVCX neurons (blue circles), HVCINT neurons (orange triangles), HVCRA neurons (purple squares) and the CSN neuron (green circle). Selective neurons are named according to what they are selective to. A for A-selective neuron, B for B-selective neuron and AB for AB-selective neuron.

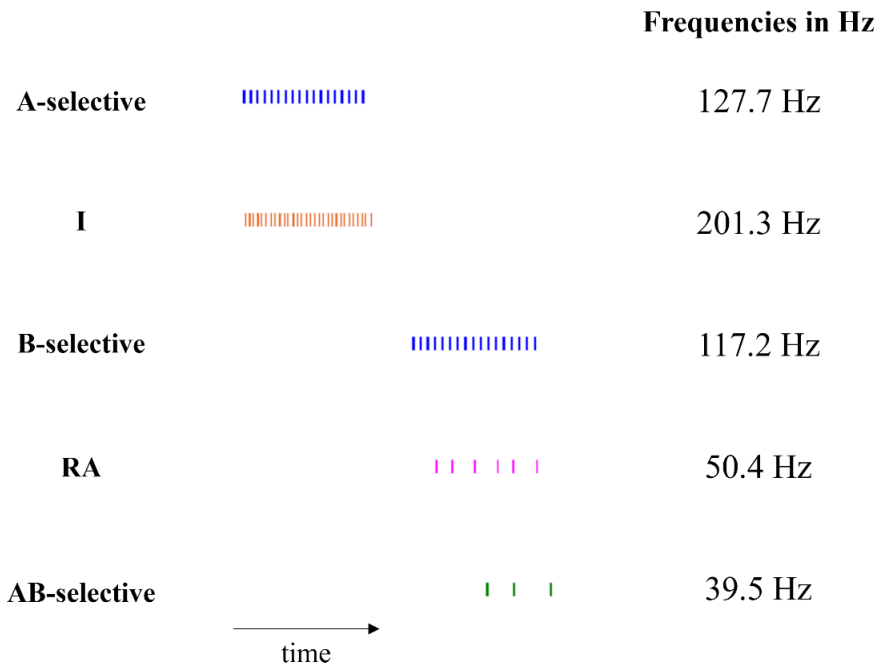

Figure 19: Raster plot depicting the firing activity for network 4 and showing the neurons' responses in time. Each tick mark in a row represents an action potential for the corresponding neuron in that row. The spikes are arranged exactly as they occur in time. Blue spikes represent HVC_X neurons' spikes, orange spikes represent HVC_{INT} neurons' spikes and meringue spikes represent HVC_{RA} neurons' spikes. The overlap of the RA firing and the post-hyperpolarization rebound depolarization of AB-selective neuron allows it to fire (see text).

2. Circuit 5: Outlasting inhibition to the HVC_{INT} neuron:

The final diagram we present in this paper relies on the fact that an interneuron fires with a much higher frequency than an HVC_{RA} neuron. This would mean that if both an inhibitory and an excitatory signal are reaching an RA neuron, the RA neuron will most likely not be able to fire due to its relatively low excitability. In this network (Fig. 20), the presentation of syllable A through the simulation of A-selective neuron will result in an excitatory signal in the neuron INT_1 to fire due to the excitatory AMPA/NMDA coupling between of INT_1 to A-selective neuron. INT_2 will be inhibited by INT_1 and when A-selective neuron stops firing, INT_1 will go back to its resting membrane potential because its excitatory drive has ended, INT_2 will no longer be inhibited and the signal will fade away before reaching the CSN which will stay silent. On the other hand, the

presentation of syllable B will send an excitatory signal down to both neurons INT_2 and RA. Since the interneuron is faster in responding to an excitatory signal then the RA-projecting neuron which usually undergoes a delay in firing before the actual response (Daou, Ross et al. 2013), INT_2 will be inhibiting RA before it has the chance to fire due to the GABAergic synaptic connection from INT_2 to RA. The signal will be stopped from propagating further and the CSN will not be receiving any signal from the network. The effect that the presentation of syllable B induces in the circuit fades away as soon as the B-selective neuron stops spiking. Therefore, when syllable B is presented and syllable A follows, the signal generated will be that of presenting B alone followed by the signal of presenting A alone. In both these latter cases the CSN is silent and therefore the CSN will not undergo a response in the case of presenting syllable B followed by syllable A. Nevertheless, when syllable A precedes syllable B, the simulation of A-selective neuron results in an excitatory signal in neuron INT_1 which inhibits INT_2 for a relatively long duration due to the very high natural excitability of interneurons. When syllable B is presented and an excitatory signal is sent down to INT_2 and RA, the inhibition from INT_1 onto INT_2 stops the INT_2 from sending an inhibitory signal onto RA for a certain period of time. This in trun allows neuron RA to send an excitatory signal to the CSN which consequently generates a response (Fig. 21).

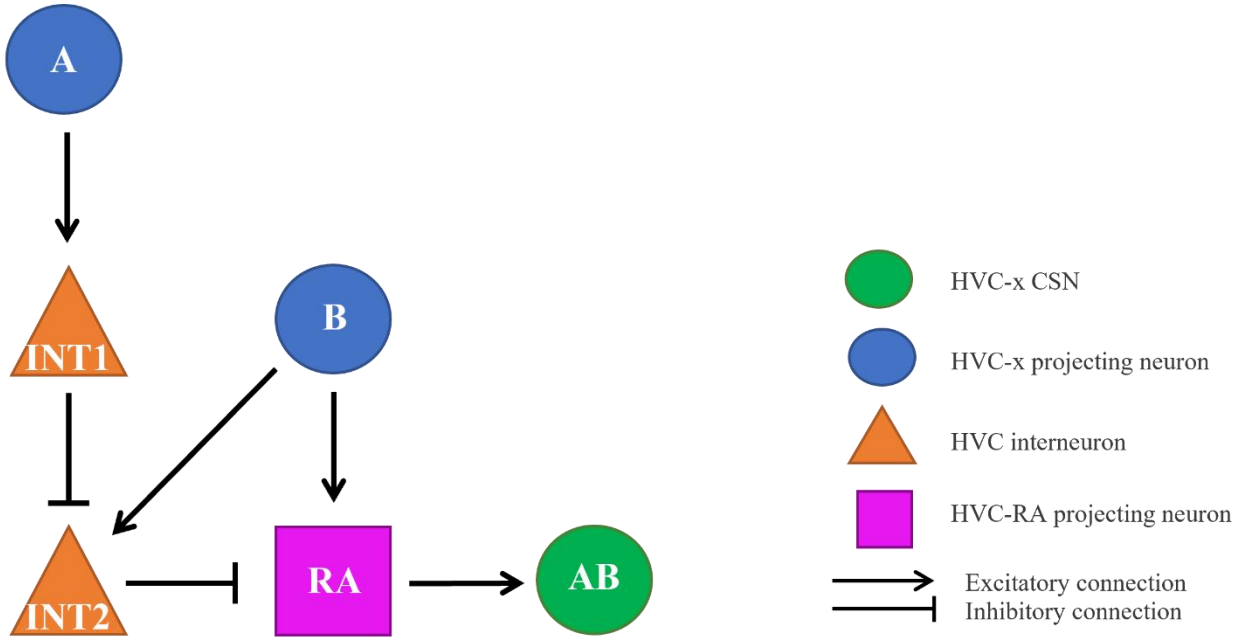

Figure 20: Network model 5 showing all different excitatory and inhibitory synaptic connections between HVCX neurons (blue circles), HVCINT neurons (orange triangles), HVCRA neurons (purple squares) and the CSN neuron (green circle). Selective neurons are named are named according to what they are selective to. A for A-selective neuron, B for B-selective neuron and AB for AB-selective neuron.

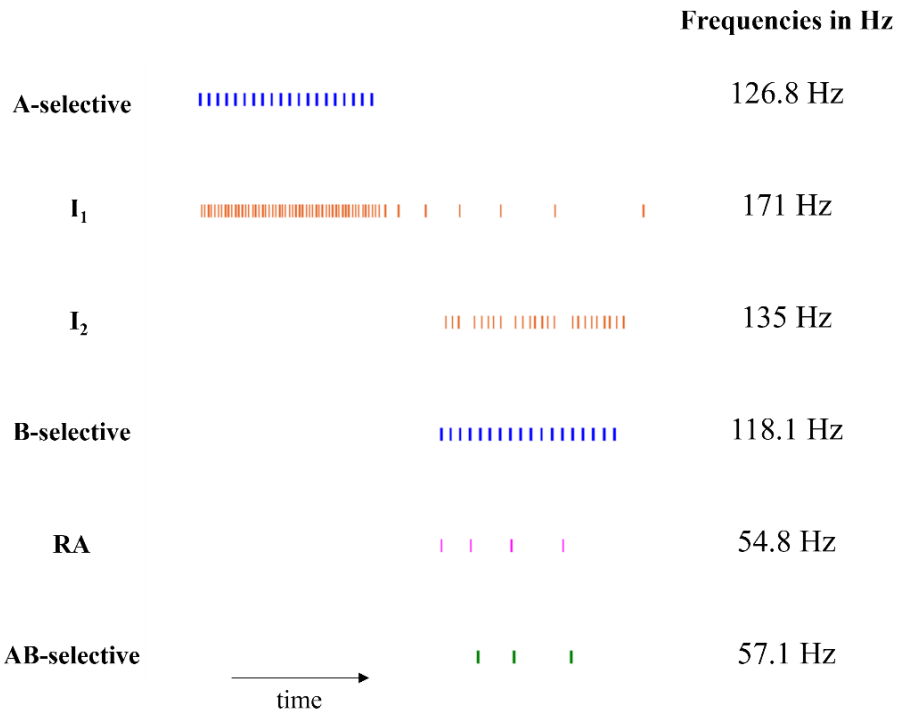

Figure 21: Raster plot depicting the firing activity for network 5 and showing the neurons' responses in time. Each tick mark in a row represents an action potential for the corresponding neuron in that row. The spikes are arranged exactly as they occur in time. Blue spikes represent HVC_X neurons' spikes, orange spikes represent HVC_{INT} neurons' spikes and meringue spikes represent HVC_{RA} neurons' spikes. The overlap of RA firing and I_2 silence allows the CSN to fire (see text).

C. Delay factor:

In order to maintain the combination sensitivity behavior for large intersyllable intervals in the models we have developed, we add one additional HVC_X neuron to the each one of the circuits with reciprocating synaptic connections between the new HVC_X neuron and an HVC_X or HVC_{INT} neuron previously present in the circuit . The purpose is to create a closed loop of continuous action potential propagation between the two neurons to keep the signal resultant from the presentation of syllable A alive until the presentation of syllable B occurs. In circuit model 1, X_3 has been added with reciprocating excitatory synaptic connections between X_3 and X_1 (Fig. 22A). As soon as X_1 fires for the first time in the network, X_3 undergoes an excitatory response as a result of the AMPA/NMDA coupling to X_2. Afterwards, X_3 sends an excitatory signal to X_1 which continues its signal generation as a result. The role of X_3 is to keep the neuron X_1 firing after the end of syllable A presentation, thereby keeping both neurons X_2 and INT_2 spiking. This ensures that there is an excitatory signal (coming from X_2) ready to excite the CSN as soon as syllable B is presented and consequently INT_2 is inhibited. We model X_3 into our network and test the output for an intersyllable interval of 350 msec. We notice that the CSN is still capable of producing a response to syllable B presentation even when it is delayed (Fig. 23A). Both neurons X_2 and INT_2 were firing continuously as a result of the new connection between neurons X_2 and X_3 (Fig. 24A). However, when B-selective neuron fired, INT_3 fired as well and inhibited INT_2 which allowed the CSN neuron to produce action potential spikes (Fig. 24A). Similar to network 1, we added an HVC_X neuron to network 1 and call it X_5 (Fig. 22B). This time, X_5 is connected to an interneuron INT_1. In this case, X_5 is inhibited by INT_1 and makes a rebound burst once it escapes the inhibition which causes INT_1 to fire again due to the excitatory connection

between X_5 and INT_1, and the closed loop of reciprocating signals between X_5 and INT_1 keeps running until syllable B is presented. Once syllable B is presented, the inhibition of INT_2 by INT_1 results in one single excitation signal to reach AB-selective neuron through the B-selective, X_2, X_3 neurons path and will the CSN fires even with an intersyllable interval of 350msec (Fig. 23B). It can be seen from Fig. 24B that the continuous firing of INT_1 resulting in the silencing of INT_2 (as can be seen from the overlap in time in the rasterplot) is the reason behind the firing of the CSN when syllable B was presented. For circuit network 3, we add a new neuron X_3 with an additional connection between neurons X_2 and X_3. This new connection creates the redundant excitation of neuron X_2 and therefore the redundant signal that inhibits X_1 in a cyclic form (Fig. 22B). When syllable B is presented after an interval of 350msec, X_1 is under a second inhibition from INT_2 which causes both the hyperpolarization activated current and T-type calcium current to be activated and results in a rebound burst in X_1. This rebound action potential generation travels down to the CSN and in turn causes an excitatory response of APs in the CSN (Fig. 23C). The additional inhibition on neuron X_1 during the period before syllable B is presented is the reason behind the post-inhibitory rebound burst that X_1 produces after the termination of the signal coming from B-selective neuron (Fig. 24C) which allows the CSN to fire.

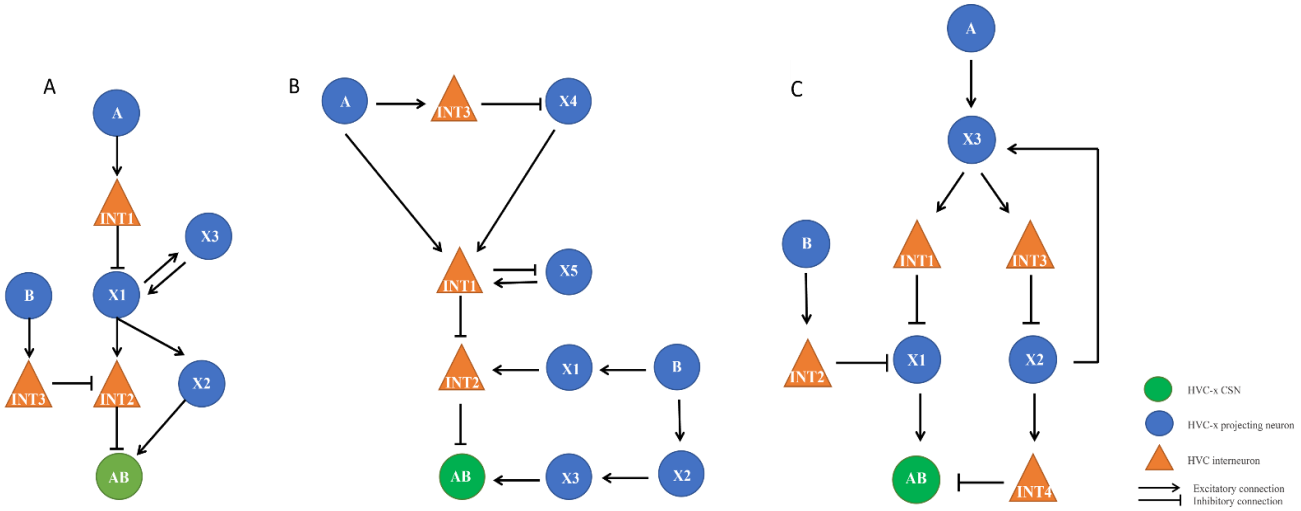

Figure 22: Schematic of the networks with a delay factor showing all different excitatory and inhibitory synaptic connections between HVCX neurons (blue circles) and HVCINT neurons (orange triangles) and the CSN neuron (green circle). Selective neurons are named according to what they are selective to. A for A-selective neuron, B for B-selective neuron and AB for AB-selective neuron *(A)* Network model 1 with additional HVC_X neuron X_3 - *(B)* Network model 2 with an additional HVC_X neuron X_5 – *(C)* Network model 3 with an additional HVC_X neuron X_3.

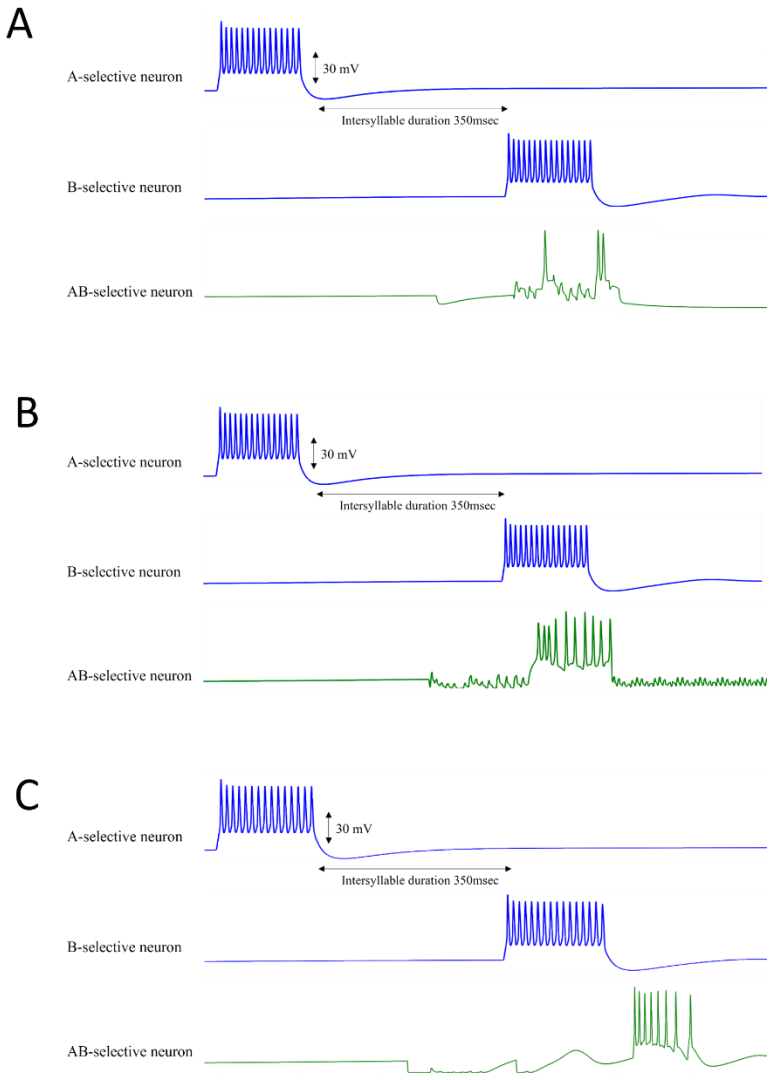

Figure 23: Action potential spiking of A-selective and B-selective and the resulting response of AB-selective neurons for an intersyllable interval between the presentation of syllable A and the presentation of syllable B of 350msec for (A) network 1, (B) network 2 and (C) network 3.

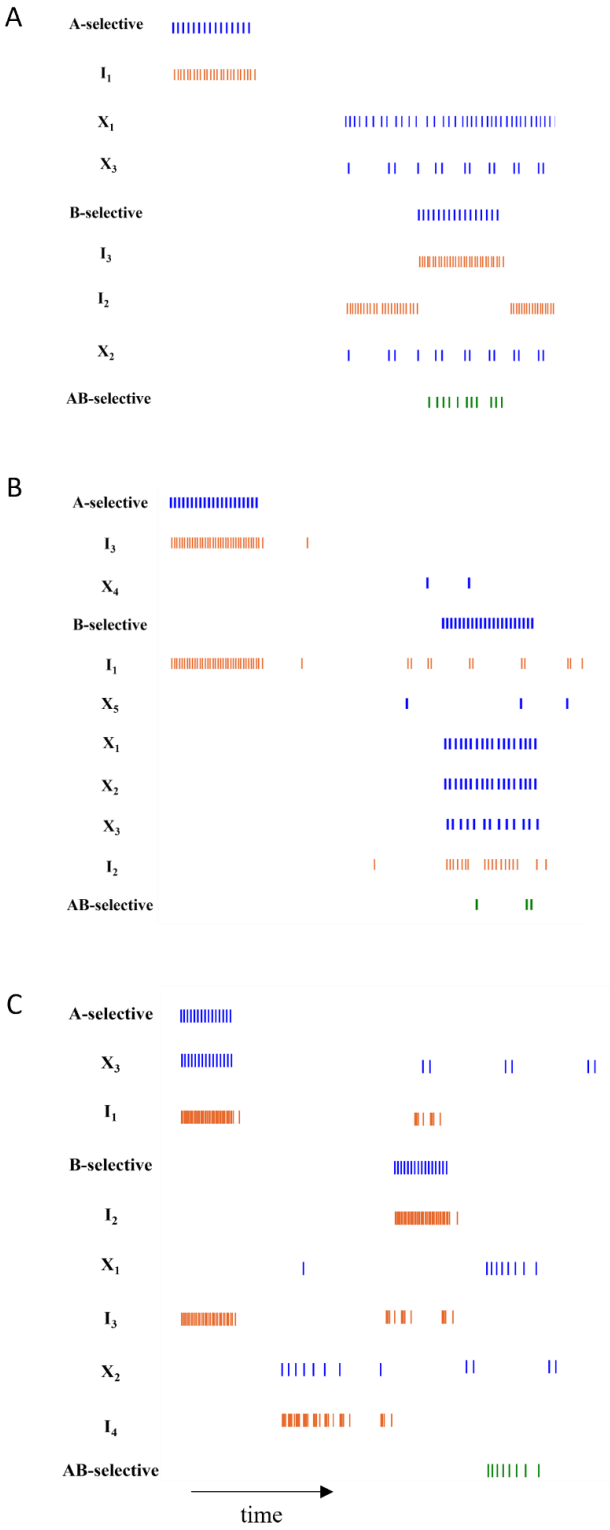

Figure 24: Raster plots depicting the firing activity for *(A)* network 1 activity with a delay factor *(B)* network 2 activity with a delay factor *(C)* network 3 activity with a delay factor - showing the neurons' responses in time. Each tick mark in a row represents an action potential for the corresponding neuron in that row. The spikes are arranged exactly as they occur in time. Blue spikes represent HVC_X neurons' spikes and orange spikes represent HVC_{INT} neurons' spikes.

D. Q factor:

When the Q factor is added to all five circuits and the temperature is increased by 10^0C, the CSN behavior changes depending on the circuit dynamics and synaptic connections. Generally, when the temperature increases, the excitability of the neurons increase. Depending on the neurons connected to the CSN, the CSN will either fire more frequently or less frequently with temperature increase. At the original temperature of the medium, a DC current imitating the presentation of the syllables of 100 msec instead of 150 msec results in different consequences depending on the network (Fig. 25). In general, the behavior of the CSN for an input syllable duration of 100msec has decreased in quality than that for the input of 150msec previously reported. In some cases, this decrease has caused a complete or partial dysfunctionality of the network (Fig.25C,E). When the temperature is now increased by 10^0C and the duration of the syllable input is chosen to be a 100msec, we notice that for some networks, the increase in temperature resulted in a better performance and a smoother pattern of action potential spikes for the CSN (Fig.25A,B,E,F). For other networks, the increase in temperature did not significantly change the output of the circuit (Fig.25G,H,I,J). In general, this is dependent on the synaptic connections between the different neurons of the network and the interplay between them which will cause the CSN to fire in a certain manner when both its excitability and the excitability of the neurons in its surrounding has increased.

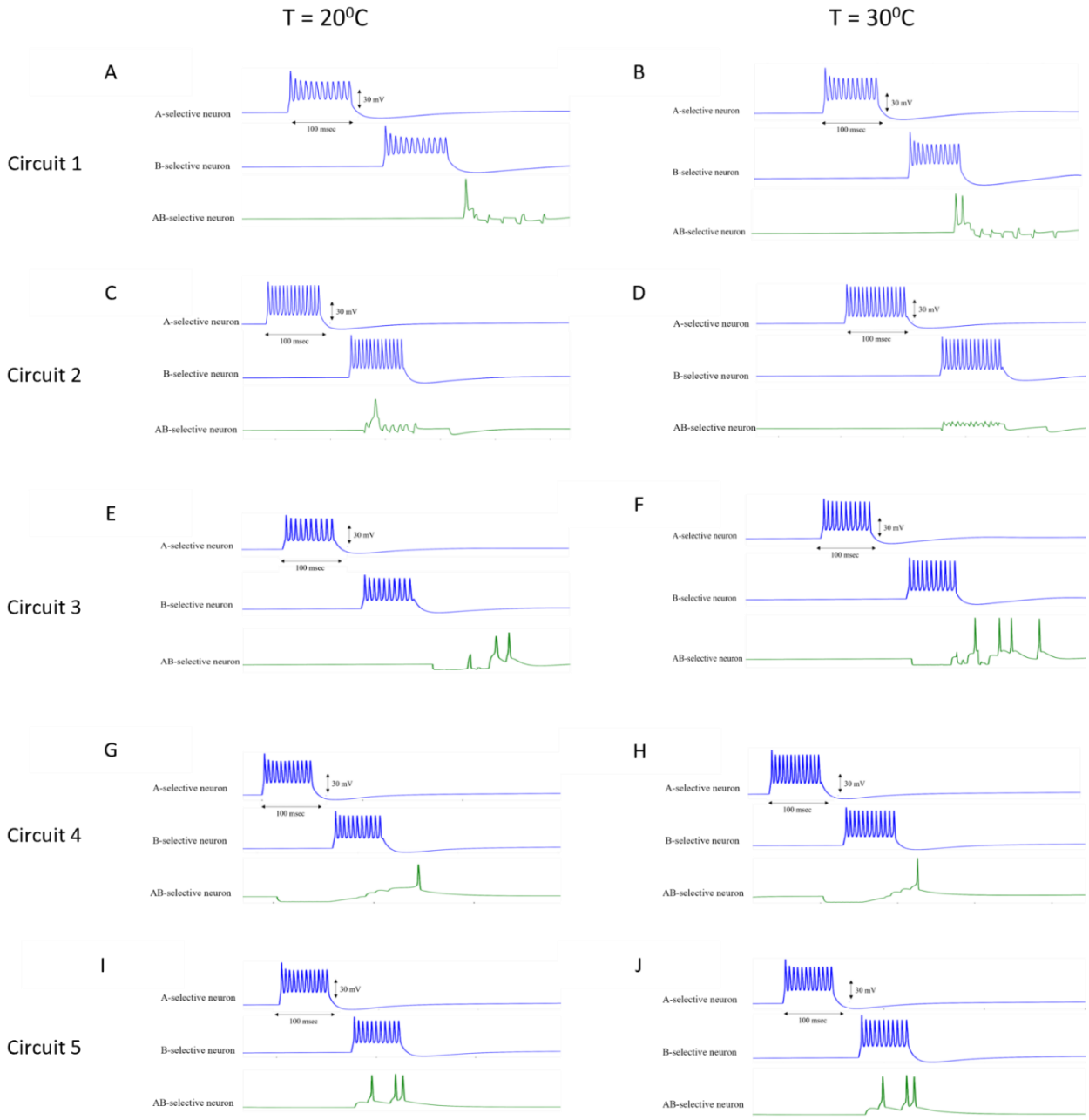

Figure 25: Action potential spikes of A-selective, B-selective and AB-selective neuron for all five circuit networks at the original temperature of T=20^{0}C (*Left column)* and at an increased temperature of T=30^{0}C (*right column)* for a decreased syllable duration of 100msec.

CHAPTER V

DISCUSSION

We have developed three different models that include HVC_X and HVC_{INT} neurons and two models that additionally include HVC_{RA} neurons. Each of the networks have its own assumptions and predictions. One assumption in circuit models 1, 2 and 5 is the arrival of an excitatory signal as well as an inhibitory signal at the synapse of a neuron at the same time will result in an additive effect of the two signals where if the two signals are opposite as in this case, they will cancel out. Similar predictions are made by (Margoliash 1983) and (Lewicki and Konishi 1995) about the selectivity emerging from the interaction (double role) of inhibition and excitation. The main assumption made in model 3 is that an inhibition that is not long enough will not cause a rebound burst. An additional period of inhibition for the same amplitude of hyperpolarizing current might be capable of activating the T-type Calcium current and hyperpolarization-activated H current and thus allow the neuron to make a rebound burst (Kopp-Scheinpflug, Tozer et al. 2011, Daou, Ross et al. 2013). Model 4 is based on the idea that HVC_{RA} neurons fire at very low frequency and therefore their excitatory signal alone is not enough to cause an EPSP in the postsynaptic neuron. All of our models would not be functional if the effect that the presentation of syllable A induces in the network does not overpast its presentation. This means that for the presentation of syllable A to effect the outcome of the presentation of syllable B, the two signals coming from each presentation alone need to overlap in time in a certain neuron in the network. This prediction has also been made previously by another model (Drew and Abbott 2002). In our case, this lasting effect is maintained by the rebounding neurons. The models also predict that there are neurons

which only fire if A is presented, even when in isolation and others that only fire when B is presented. Their selective responses may be in the form of a hyperpolarization or a depolarization.

These models rely heavily on the role of inhibitory neurons. In fact, the role of inhibition has been commonly studied for similar purposes. Inhibition is one way for neurons to of code for temporal durations (Sun, Zhang et al. 2020). Lewicki and Konishi 1995 note that the inhibition on HVC_X neurons might be essential for the syllable sequences sensitivity generation. It is also noted that almost every HVC_X neuron undergoes hyperpolarization during the song and that interneurons' spikes are frequently accompanied with HVC_X hyperpolarizations (Mooney 2000). Solis and Perkel 2005 state that the timing and presence of rhythmic activity is governed by inhibition and that therefore, an internal HVC circuitry is present and is grounds for pattern generation. Additionally, it has been also discussed that interneurons' activity which is the basis of HVC rhythm, arises from reciprocal connections between interneurons and the excitatory cells (Solis and Perkel 2005). In our model networks, almost every HVC_X neuron present is receiving hyperpolarizing input from an HVC_{INT} neuron during the syllables presentation. This is supported by all the experimental conclusions reached in earlier studies.

In these circuit models, several realistic aspects were meant to be preserved. We know from literature that the CSN does not fire at a specific time once the second syllable is presented. Margoliash and Fortune 1992 note that the CSN fires sometimes at the onset of syllable B, sometimes in the middle and other times at the offset. For the different models presented in this paper, the CSN will be firing at a different point in time;

sometimes at the onset (models 1 and 5) in the middle (models 1, 2 and 4) or at the offset (model 3) of the presentation of the second syllable. This means that different circuitries can explain the different behaviors and the presence of many different networks in real life is possible. Also, the biological circuitries might be more flexible than those created with this model. Thus the same circuit in reality might have a bigger and more flexible margin for the response of the CSN.

Another feature that we tried to take into consideration was the steadiness of the CSN in case of the same syllable presented many times; such as the presentation of syllables A-A-A or B-B-B and so on. According to research, these combinations of the same syllable do not induce a response in the CSN (Lewicki and Konishi 1995, Lewicki and Arthur 1996). Margoliash 1983 proposed a model that relies on the rebound of inhibition caused by syllable A and an excitation caused by syllable B happening at the same time. However, in this model, one would expect to get a CSN response for B-B combination of input (Lewicki and Konishi 1995). In the case of circuit models 1, 2 and 5, no response is to be expected from these type of combinations because for either syllable, we have solely two possible scenarios. The first scenario is that the syllable causes an inhibition always accompanied by an excitation (syllable B in networks 1 and 5 and syllable A in network 2). Regardless of how many times the syllable is presented, the signals will always cancel out. The second scenario is that only an inhibitory signal is present (syllable A in networks 1 and 5 and syllable B in network 2). In circuit models 3 and 4, a combination of syllable A and/or a combination of syllable B presentations might induce a response since additional inhibition might result in rebound bursts that will become postsynaptic excitatory signals in the CSN. However, this is not completely far from the

biophysical features of the CSN because Lewicki and Arthur 1996 report slight response in the CSN for A-A combinations and marginally stronger responses B-B combinations.

The delay in the first three circuit models was implemented by adding a connection between two neurons that excite each other either directly or by consecutive excitation and inhibition that causes rebound bursts. This implementation assumes that after some time - precisely, the time after which the presentation of B no longer induces a response in the CSN - even if syllable B was not presented, the neurons' signal shall fade away by itself. This also implies that some HVC_X neurons will burst multiple times until syllable B has been presented. This is supported by an observation made by the Kohzevnikov and Fee 2007 study where the data reported supports the idea that bursts of an HVC_X neuron seem to precede elements of the syllable pattern and does not have to do with similar acoustic elements of the song. A delay factor was not implemented in the last couple of networks where HVC_{RA} neurons were integrated. That is due to the fact that a delay factor would force the multiple firing of the neurons in the circuit while HVC_{RA} neurons fire only one time during the song rendition (Hahnloser, Kozhevnikov et al. 2002). Therefore, a delay factor of the same nature used in this paper would not be biophysically realistic.

CHAPTER VI

CONCLUSION

Analysis of auditory information for the creation of appropriate responses is a very precise and detailed process with many largely unknown aspects; combination-sensitivity property being one of them. In this paper, we have sketched hypothetical circuit networks connecting either two or all three classes of the neurons in the HVC nucleus of songbirds based on realistic features of the neurons in order to explain combination-sensitivity. These sketches were then turned into biophysically plausible models of neurons and synaptic connections between them that are Hodgkin-Huxley based models taking into consideration the different classes and their diverse but identified ionic currents. Each one of the circuits presented revolved around specific circuit dynamics and intrinsic neuronal features that combined, would give rise to combination-sensitive neurons in different ways. The networks also differ in how biophysically realistic and accurate each is and in the essential features that allow the functionality of the network.

Additionally, we note the effect of temperature change of the medium on the different circuit dynamics while varying the syllable input duration in order to see the correlation between the excitability of the neurons and the shortest syllable duration necessary for the production of the combination-sensitivity property. For the first three diagrams, we were able to add a delay factor that is represented by a ‘while loop’ of reciprocating synaptic connections between two neurons that will keep each other firing and waiting for the presentation of the second syllable.

The models presented here are very realistic and in accordance with not only the HVC nucleus and the different properties of different neuronal classes in it, but also with the behavior of neural networks in general and the role of multiple excitations, inhibition and of temporal summation. Therefore, it would be necessary to validate these networks in the future by developing the right experimental strategy that allows testing of the presence of a certain wiring diagram in the HVC nucleus.

Despite the fact that we proved in this paper that there might exist many different wiring networks of connected neurons that will produce combination sensitivity behavior, it would still be important to check which of these networks would still be functional for longer sequences of three and more syllables presentations. As previously noted, some neurons are sensitive to the sequence of syllables that covers the whole BOS of the bird. It is therefore important to check the effect of the number of elements within the series on the circuit and what it would entail.

REFERENCES

Bottjer, S. W., et al. (1989). "Axonal connections of a forebrain nucleus involved with vocal learning in zebra finches." Journal of Comparative Neurology **279**(2): 312-326.

Brainard, M. S. and A. J. Doupe (2002). "What songbirds teach us about learning." Nature **417**(6886): 351-358.

Brenowitz, E. A., et al. (1997). "An introduction to birdsong and the avian song system." Journal of neurobiology **33**(5): 495-500.

Capranica, R. R. (1965). THE EVOKED VOCAL RESPONSE OF THE BULLFROG; A STUDY OF COMMUNICATION BY SOUND, MASSACHUSETTS INST OF TECH CAMBRIDGE RESEARCH LAB OF ELECTRONICS.

Cardin, J. A. and M. F. Schmidt (2004). "Noradrenergic inputs mediate state dependence of auditory responses in the avian song system." Journal of Neuroscience **24**(35): 7745-7753.

Carr, C. and M. Konishi (1990). "A circuit for detection of interaural time differences in the brain stem of the barn owl." Journal of Neuroscience **10**(10): 3227-3246.

Cash, S. and R. Yuste (1998). "Input summation by cultured pyramidal neurons is linear and position-independent." Journal of Neuroscience **18**(1): 10-15.

Daou, A. and D. Margoliash (2020). "Intrinsic neuronal properties represent song and error in zebra finch vocal learning." Nature communications **11**(1): 1-17.

Daou, A. and D. Margoliash (2021). "Intrinsic plasticity and birdsong learning." Neurobiology of Learning and Memory **180**: 107407.

Daou, A., et al. (2013). "Electrophysiological characterization and computational models of HVC neurons in the zebra finch." Journal of neurophysiology **110**(5): 1227-1245.

Doupe, A. J. (1997). "Song-and order-selective neurons in the songbird anterior forebrain and their emergence during vocal development." Journal of Neuroscience **17**(3): 1147-1167.

Doupe, A. J. and M. Konishi (1991). "Song-selective auditory circuits in the vocal control system of the zebra finch." Proceedings of the National Academy of Sciences **88**(24): 11339-11343.

Doupe, A. J. and P. K. Kuhl (1999). "Birdsong and human speech: common themes and mechanisms." Annual review of neuroscience **22**(1): 567-631.

Drew, P. J. and L. Abbott (2002). "Modeling temporal combination selective neurons of the songbird." Neurocomputing **44**: 789-794.

Dutar, P., et al. (1998). "Multiple cell types distinguished by physiological, pharmacological, and anatomic properties in nucleus HVc of the adult zebra finch." Journal of neurophysiology **80**(4): 1828-1838.

Fee, M. S., et al. (2004). "Neural mechanisms of vocal sequence generation in the songbird." Annals of the New York Academy of Sciences **1016**(1): 153-170.

Foster, E. F., et al. (1997). "Axonal connections of the medial magnocellular nucleus of the anterior neostriatum in zebra finches." Journal of Comparative Neurology **382**(3): 364-381.

Fujimoto, H., et al. (2011). "Neural coding of syntactic structure in learned vocalizations in the songbird." Journal of Neuroscience **31**(27): 10023-10033.

Fuzessery, Z. and J. Hall (1996). "Role of GABA in shaping frequency tuning and creating FM sweep selectivity in the inferior colliculus." Journal of neurophysiology **76**(2): 1059-1073.

Fuzessery, Z. M. and A. S. Feng (1982). "Frequency selectivity in the anuran auditory midbrain: single unit responses to single and multiple tone stimulation." Journal of comparative physiology **146**(4): 471-484.

Fuzessery, Z. M. and A. S. Feng (1983). "Mating call selectivity in the thalamus and midbrain of the leopard frog (Rana p. pipiens): single and multiunit analyses." Journal of comparative physiology **150**(3): 333-344.

Griffin, D. R. (1958). "Listening in the dark: the acoustic orientation of bats and men."

Gritti, I., et al. (2003). "Parvalbumin, calbindin, or calretinin in cortically projecting and GABAergic, cholinergic, or glutamatergic basal forebrain neurons of the rat." Journal of Comparative Neurology **458**(1): 11-31.

Gulyás, A. I., et al. (1996). "Interneurons containing calretinin are specialized to control other interneurons in the rat hippocampus." Journal of Neuroscience **16**(10): 3397-3411.

Hahnloser, R. H., et al. (2002). "An ultra-sparse code underliesthe generation of neural sequences in a songbird." Nature **419**(6902): 65-70.

Heiligenberg, W., et al. (1978). "The jamming avoidance response inEigenmannia revisited: The structure of a neuronal democracy." Journal of comparative physiology **127**(3): 267-286.

Hyngstrom, A. S., et al. (2008). "Summation of excitatory and inhibitory synaptic inputs by motoneurons with highly active dendrites." Journal of neurophysiology **99**(4): 1643-1652.

Kanwal, J. S., et al. (1994). "Analysis of acoustic elements and syntax in communication sounds emitted by mustached bats." The Journal of the Acoustical Society of America **96**(3): 1229-1254.

Katz, L. C. and M. E. Gurney (1981). "Auditory responses in the zebra finch's motor system for song." Brain research **221**(1): 192-197.

Knudsen, E. I. and M. Konishi (1978). "A neural map of auditory space in the owl." Science **200**(4343): 795-797.

Knudsen, E. I. and M. Konishi (1979). "Mechanisms of sound localization in the barn owl (Tyto alba)." Journal of comparative physiology **133**(1): 13-21.

Konishi, M. (1965). "The role of auditory feedback in the control of vocalization in the white-crowned sparrow 1." Zeitschrift für Tierpsychologie **22**(7): 770-783.

Kopp-Scheinpflug, C., et al. (2011). "The sound of silence: ionic mechanisms encoding sound termination." Neuron **71**(5): 911-925.

Kosche, G., et al. (2015). "Interplay of inhibition and excitation shapes a premotor neural sequence." Journal of Neuroscience **35**(3): 1217-1227.

Kozhevnikov, A. A. and M. S. Fee (2007). "Singing-related activity of identified HVC neurons in the zebra finch." Journal of neurophysiology **97**(6): 4271-4283.

Kubota, M. and N. Saito (1991). "Sodium-and calcium-dependent conductances of neurones in the zebra finch hyperstriatum ventrale pars caudale in vitro." The Journal of physiology **440**(1): 131-142.

Kubota, M. and I. Taniguchi (1998). "Electrophysiological characteristics of classes of neuron in the HVc of the zebra finch." Journal of neurophysiology **80**(2): 914-923.

Léger, J.-F., et al. (2005). "Synaptic integration in rat frontal cortex shaped by network activity." Journal of neurophysiology **93**(1): 281-293.

Lewicki, M. S. (1996). "Intracellular characterization of song-specific neurons in the zebra finch auditory forebrain." Journal of Neuroscience **16**(18): 5854-5863.

Lewicki, M. S. and B. J. Arthur (1996). "Hierarchical organization of auditory temporal context sensitivity." Journal of Neuroscience **16**(21): 6987-6998.

Lewicki, M. S. and M. Konishi (1995). "Mechanisms underlying the sensitivity of songbird forebrain neurons to temporal order." Proceedings of the National Academy of Sciences **92**(12): 5582-5586.

Liberman, A. M., et al. (1981). "Duplex perception of cues for stop consonants: Evidence for a phonetic mode." Perception & Psychophysics **30**(2): 133-143.

Long, M. A., et al. (2010). "Support for a synaptic chain model of neuronal sequence generation." Nature **468**(7322): 394-399.

Luo, M. and D. J. Perkel (1999). "A GABAergic, strongly inhibitory projection to a thalamic nucleus in the zebra finch song system." Journal of Neuroscience **19**(15): 6700-6711.

Margoliash, D. (1983). "Acoustic parameters underlying the responses of song-specific neurons in the white-crowned sparrow." Journal of Neuroscience **3**(5): 1039-1057.

Margoliash, D. (1986). "Preference for autogenous song by auditory neurons in a song system nucleus of the white-crowned sparrow." Journal of Neuroscience **6**(6): 1643-1661.

Margoliash, D. and E. S. Fortune (1992). "Temporal and harmonic combination-sensitive neurons in the zebra finch's HVc." Journal of Neuroscience **12**(11): 4309-4326.

Margulis, M. and C.-M. Tang (1998). "Temporal integration can readily switch between sublinear and supralinear summation." Journal of neurophysiology **79**(5): 2809-2813.

Marler, P. (1970). "A comparative approach to vocal learning: song development in white-crowned sparrows." Journal of comparative and physiological psychology **71**(2p2): 1.

McCasland, J. S. (1987). "Neuronal control of bird song production." Journal of Neuroscience **7**(1): 23-39.

Mittmann, D. H. and J. J. Wenstrup (1995). "Combination-sensitive neurons in the inferior colliculus." Hearing research **90**(1-2): 185-191.

Mooney, R. (2000). "Different subthreshold mechanisms underlie song selectivity in identified HVc neurons of the zebra finch." Journal of Neuroscience **20**(14): 5420-5436.

Mooney, R. (2009). "Neural mechanisms for learned birdsong." Learning & memory **16**(11): 655-669.

Mooney, R., et al. (2001). "Auditory representation of the vocal repertoire in a songbird with multiple song types." Proceedings of the National Academy of Sciences **98**(22): 12778-12783.

Mooney, R. and J. F. Prather (2005). "The HVC microcircuit: the synaptic basis for interactions between song motor and vocal plasticity pathways." Journal of Neuroscience **25**(8): 1952-1964.

Nataraj, K. and J. J. Wenstrup (2005). "Roles of inhibition in creating complex auditory responses in the inferior colliculus: facilitated combination-sensitive neurons." Journal of neurophysiology **93**(6): 3294-3312.

Nottebohm, F., et al. (1982). "Connections of vocal control nuclei in the canary telencephalon." Journal of Comparative Neurology **207**(4): 344-357.

Nottebohm, F., et al. (1976). "Central control of song in the canary, Serinus canarius." Journal of Comparative Neurology **165**(4): 457-486.

O'Neill, W. E. and N. Suga (1982). "Encoding of target range and its representation in the auditory cortex of the mustached bat." Journal of Neuroscience **2**(1): 17-31.

O'Leary, T. and E. Marder (2016). "Temperature-robust neural function from activity-dependent ion channel regulation." Current Biology **26**(21): 2935-2941.

Powers, R. K. and M. D. Binder (2000). "Summation of effective synaptic currents and firing rate modulation in cat spinal motoneurons." Journal of neurophysiology **83**(1): 483-500.

Prather, J. F., et al. (2001). "Amplification and linear summation of synaptic effects on motoneuron firing rate." Journal of neurophysiology **85**(1): 43-53.

Rauschecker, J. P., et al. (1995). "Processing of complex sounds in the macaque nonprimary auditory cortex." Science **268**(5207): 111-114.

Rubel, E. W., et al. (1976). "Organization and development of brain stem auditory nuclei of the chicken: ontogeny of n. magnocellularis and n. laminaris." Journal of Comparative Neurology **166**(4): 469-489.

Schmidt, M. F. and D. J. Perkel (1998). "Slow synaptic inhibition in nucleus HVc of the adult zebra finch." Journal of Neuroscience **18**(3): 895-904.

Shea, S. D., et al. (2010). "Neuron-specific cholinergic modulation of a forebrain song control nucleus." Journal of neurophysiology **103**(2): 733-745.

Slater, P. J., et al. (1988). Song learning in zebra finches (Taeniopygia guttata): progress and prospects. Advances in the Study of Behavior, Elsevier. **18:** 1-34.

Snyder, J. S., et al. (2012). "Attention, awareness, and the perception of auditory scenes." Frontiers in psychology **3**: 15.

Solis, M. M. and A. J. Doupe (1997). "Anterior forebrain neurons develop selectivity by an intermediate stage of birdsong learning." Journal of Neuroscience **17**(16): 6447-6462.

Solis, M. M. and D. J. Perkel (2005). "Rhythmic activity in a forebrain vocal control nucleus in vitro." Journal of Neuroscience **25**(11): 2811-2822.

Stevens, S. S. and E. B. Newman (1936). "The localization of actual sources of sound." The American journal of psychology **48**(2): 297-306.

Suga, N., et al. (1983). "Specificity of combination-sensitive neurons for processing of complex biosonar signals in auditory cortex of the mustached bat." Journal of neurophysiology **49**(6): 1573-1626.

Sun, H., et al. (2020). "Developmentally regulated rebound depolarization enhances spike timing precision in auditory midbrain neurons." Frontiers in Cellular Neuroscience **14**: 236.

Sutter, M. L. and D. Margoliash (1994). "Global synchronous response to autogenous song in zebra finch HVc." Journal of neurophysiology **72**(5): 2105-2123.

Theunissen, F. E. and A. J. Doupe (1998). "Temporal and spectral sensitivity of complex auditory neurons in the nucleus HVc of male zebra finches." Journal of Neuroscience **18**(10): 3786-3802.

Theunissen, F. E. and S. S. Shaevitz (2006). "Auditory processing of vocal sounds in birds." Current opinion in neurobiology **16**(4): 400-407.

Vicario, D. S. (1991). "Organization of the zebra finch song control system: functional organization of outputs from nucleus robustus archistriatalis." Journal of Comparative Neurology **309**(4): 486-494.

Vicario, D. S. and F. Nottebohm (1988). "Organization of the zebra finch song control system: I. Representation of syringeal muscles in the hypoglossal nucleus." Journal of Comparative Neurology **271**(3): 346-354.

Vicario, D. S. and H. B. Simpson (1995). "Electrical stimulation in forebrain nuclei elicits learned vocal patterns in songbirds." Journal of neurophysiology **73**(6): 2602-2607.

Volman, S. (1996). "Quantitative assessment of song-selectivity in the zebra finch “high vocal center”." Journal of Comparative Physiology A **178**(6): 849-862.

Vu, E. T., et al. (1994). "Identification of a forebrain motor programming network for the learned song of zebra finches." Journal of Neuroscience **14**(11): 6924-6934.

Wang, X., et al. (1995). "Representation of a species-specific vocalization in the primary auditory cortex of the common marmoset: temporal and spectral characteristics." Journal of neurophysiology **74**(6): 2685-2706.

Wang, Y., et al. (2010). "Laminar and columnar auditory cortex in avian brain." Proceedings of the National Academy of Sciences **107**(28): 12676-12681.

Wessel, R., et al. (1999). "Supralinear summation of synaptic inputs by an invertebrate neuron: dendritic gain is mediated by an “inward rectifier” K+ current." Journal of Neuroscience **19**(14): 5875-5888.

Wild, J. M. (1997). "Neural pathways for the control of birdsong production." Journal of neurobiology **33**(5): 653-670.

Wild, J. M., et al. (2005). "Calcium-binding proteins define interneurons in HVC of the zebra finch (Taeniopygia guttata)." Journal of Comparative Neurology **483**(1): 76-90.

Yu, A. C. and D. Margoliash (1996). "Temporal hierarchical control of singing in birds." Science **273**(5283): 1871-1875.